สำนักหอสมุดกลาง พระจอมเกล้าลาดกระบัง

MODIFICATION OF USED ATOMIC FORCE MICROSCOPE CANTILEVER BY CARBON NANOTUBE ATTACHMENT AND ITS IMAGING PERFORMANCE

E076549

YUWAPAN MANEERAT

เลขหมู่..............................
เลขทะเบียน 76549
วัน,เดือน,ปี 26 ส.ค. 2557

b. [illegible]
i. ....

A THESIS SUBMITTED IN PARTIAL FULFILLMENT

OF THE REQUIREMENT FOR THE DEGREE OF

MASTER OF ENGINEERING IN DATA STORAGE TECHNOLOGY

INTERNATIONAL COLLEGE

KING MONGKUT'S INSTITUTE OF TECHNOLOGY LADKRABANG

2013

KMITL-2013-IC-M-005-005

This material is reserved for educational use only, not allowed for commercial use.
Forbidden to modify the content, and cite the document when use.

COPYRIGHT 2013

INTERNATIONAL COLLEGE

KING MONGKUT'S INSTITUTE OF TECHNOLOGY LADKRABANG

This material is reserved for educational use only, not allowed for commercial use.

Forbidden to modify the content, and cite the document when use.

หัวข้อวิทยานิพนธ์	การปรับปรุงเข็มของกล้องจุลทรรศน์แรงอะตอมที่ใช้แล้วด้วยท่อนาโนคาร์บอนและศึกษาประสิทธิภาพการแสกนภาพ
นักศึกษา	นางสาวยุวพันธ์ มณีรัตน์
รหัสประจำตัว	53600624
ปริญญา	วิศวกรรมศาสตรมหาบัณฑิต
สาขาวิชา	เทคโนโลยีการบันทึกข้อมูล
พ.ศ.	2556
อาจารย์ที่ปรึกษาวิทยานิพนธ์	ดร.วินัดดา วงศ์วิริยะพันธ์

บทคัดย่อ

เข็มกล้องจุลทรรศน์แรงอะตอม (AFM) ที่ผ่านการใช้งานแล้ว ได้รับการปรับปรุงนำกลับมาใช้ใหม่ด้วยการติดท่อนาโนคาร์บอนที่ปลายเข็มและสาธิตประสิทธิภาพการแสกนภาพของเข็มท่อนาโนคาร์บอน การติดท่อนาโนคาร์บอนที่ปลายเข็ม AFM ทำด้วยวิธีการสังเคราะห์แบบการตกระเหยทางเคมีด้วยความร้อน โดยใช้นิกเกิลเป็นโลหะคะตะลิสต์และใช้แอลกอฮอล์เป็นแหล่งกำเนิดคาร์บอน เข็ม AFM ที่นำมาใช้ทำมาจากซิลิกอน การเตรียมฟิล์มนิกเกิลบนปลายเข็ม AFM ที่มีรูปร่างเป็นทรงปิรามิดนั้น ทำด้วยวิธีชุบทางไฟฟ้า เงื่อนไขสำหรับการสังเคราะห์ท่อนาโนคาร์บอนบนเข็ม AFM ที่ดีที่สุด คือการเตรียมฟิล์มนิกเกิลโดยใช้อุณหภูมิของน้ำยาชุบนิกเกิลที่ 40 องศา เป็นเวลา 6 วินาที ภายใต้ความต่างศักย์ไฟฟ้า 1.4 โวลต์ กระแสไฟฟ้า 0.01 แอมแปร์ ระยะห่างระหว่างขั้วบวกและขั้วลบ 13 เซนติเมตร และเงื่อนไขการตกระเหยทางเคมีด้วยความร้อนที่อุณหภูมิ 850 องศาเป็นเวลา 20 นาที การวิเคราะห์ท่อนาโนคาร์บอนที่สังเคราะห์บนเข็ม AFM ทำด้วยเทคนิคกล้องจุลทรรศน์อิเล็กตรอนแบบส่องกราด กล้องจุลทรรศน์อิเล็กตรอนแบบส่องผ่าน และรามานสเปคโตรสโคปี พบว่าที่ปลายเข็มมีท่อนาโนคาร์บอนอยู่จำนวน 1-2 ท่อ ความยาวประมาณ 465 นาโนเมตร และเส้นผ่าศูนย์กลางประมาณ 17.29 นาโนเมตร ท่อนาโนทิวบ์มีโครงสร้างแบบผนังหลายชั้น สำหรับการสาธิตประสิทธิภาพการแสกนภาพของเข็ม AFM ท่อนาโนคาร์บอน ตัวอย่างแสกนที่ใช้คือซิลิกอนไดออกไซด์ที่เคลือบด้วยชั้นของแพลตตินัมซึ่งเป็นตัวอย่างมาตรฐานสำหรับ AFM ผลการแสกนภาพปรากฏว่าภาพและไลน์โปรไฟล์ที่ได้จากเข็ม AFM ท่อนาโนคาร์บอน ให้ความคมชัดและความละเอียด

This material is reserved for educational use only, not allowed for commercial use.
Forbidden to modify the content, and cite the document when use.

ของภาพดีกว่าทั้งเข็ม AFM ใช้งานแล้ว และเข็ม AFM ใหม่ ทั้งในแนวแกนนอนและแนวแกนตั้งของภาพแสกน

This material is reserved for educational use only, not allowed for commercial use.
Forbidden to modify the content, and cite the document when use.

Thesis	Modification of Used Atomic Force Microscope Cantilever by Carbon Nanotube Attachment and its Imaging Performance
Student	Ms. Yuwapan Maneerat
Student ID.	53600624
Degree	Master of Engineering
Program	Data Storage Technology
Year	2013
Thesis Advisor	Dr.Winadda Wongwiriyapan

ABSTRACT

Modification of used atomic force microscope (AFM) cantilever by carbon nanotube (CNT) attachment and its imaging performance was demonstrated. CNTs were directly grown on the apex of used Si AFM cantilevers by Ni catalyst-assisted chemical vapor deposition (CVD) using ethanol as the carbon source. The Ni catalyst film was deposited on the pyramid shape of the cantilever by the electroplating method. To obtain CNTs protruding from the apex, the electroplating was performed at the optimal condition with Ni plating solution temperature of 40°C for 6 s at the applied voltage of 1.4 V, current of 0.01 A and the distance between anode and cathode of 13 cm. The CVD was operated at the optimal growth temperature of 850°C for 20 min. The field-emission electron microscope, the transmission electron microscope and the Raman spectrometer were utilized for the characterization of the synthesized CNTs. There were 1-2 of thin tubular structures protruding from the apex of cantilever with the length of approximately 465 nm and the diameter of approximately 17.29 nm. The synthesized CNT were multi-walled carbon nanotube structure. For the imaging performance test, the AFM standard sample of

This material is reserved for educational use only, not allowed for commercial use.
Forbidden to modify the content, and cite the document when use.

micro-patterned Pt films on silicon dioxide was used as a test sample. Superior to new and used AFM cantilevers, the CNT-modified AFM cantilevers exhibit high-resolution imaging in both lateral and vertical resolution.

This material is reserved for educational use only, not allowed for commercial use.
Forbidden to modify the content, and cite the document when use.

ACKNOWLEDGEMENTS

First of all, I would like to thank my advisor Dr. Winadda Wongwiriyapan for her all suggestions on this research. I also would like to thank Dr. Sirapat Pratontep for his recommendation about this research.

I would like to acknowledge HGSA Failure Analysis Laboratory, Seagate (Thailand) Co., Ltd. (KORAT) for the AFM facilities, used cantilevers, AFM standard sample supports and FESEM machine for characterization.

This work has partially supported by the National Nanotechnology Center (NANOTEC), NSTDA, Ministry of Science and Technology, Thailand, through its program of Center of Excellence Network.

I also acknowledge the financial support through Master Degree Program Development in HDD Engineering Technology, NSTDA-KMITL-SEAGATE.

I would like to thank Assoc. Prof. Dr. Vittaya Amornkitbamrun and Ms. Phikun Ratphonsan, KhonKaen University for their partly assistance in high resolution transmission electron microscopy observation. I also thank to Dr.Rachsak Sakdanuphab, College of Data Storage Innovation, KMITL for atomic force microscopy advising.

Finally, I would like to thank moral support from my mother, my father and my family.

Yuwapan Maneerat

This material is reserved for educational use only, not allowed for commercial use.
Forbidden to modify the content, and cite the document when use.

TABLE OF CONTENTS

Page

This material is reserved for educational use only, not allowed for commercial use.
Forbidden to modify the content, and cite the document when use.

TABLE OF CONTENTS (CONTINUE)

Page

This material is reserved for educational use only, not allowed for commercial use.
Forbidden to modify the content, and cite the document when use.

TABLE OF CONTENTS (CONTINUE)

Page

This material is reserved for educational use only, not allowed for commercial use.
Forbidden to modify the content, and cite the document when use.

LIST OF TABLE

This material is reserved for educational use only, not allowed for commercial use.
Forbidden to modify the content, and cite the document when use.

LIST OF TABLE (CONTINUE)

Table Page

This material is reserved for educational use only, not allowed for commercial use.
Forbidden to modify the content, and cite the document when use.

LIST OF FIGURE

Figure **Page**

This material is reserved for educational use only, not allowed for commercial use.
Forbidden to modify the content, and cite the document when use.

LIST OF FIGURE (CONTINUE)

Figure **Page**

This material is reserved for educational use only, not allowed for commercial use.
Forbidden to modify the content, and cite the document when use.

LIST OF FIGURE (CONTINUE)

Figure **Page**

This material is reserved for educational use only, not allowed for commercial use.
Forbidden to modify the content, and cite the document when use.

CHAPTER 1

INTRODUCTION

1.1 Background and Problem

Atomic force microscopy or AFM is a technique for surface analysis such as surface topology and there are many applications in several industries such as data storage, semiconductors and coating. It uses mechanical force interaction between tip and sample for surface imaging. Imaging resolution determines by tip geometry. Conventional cantilever is Si cantilever with a sharp pyramidal tip. The resolution of AFM imaging depend on tip sharpness, it is necessary to develop a novel cantilever with a sharp apex to obtain the high resolution image [1]. Nowadays, there are ongoing efforts of design and manufacturing of novel cantilever by utilization of nanomaterials such as carbon nanotube [2].

Carbon nanotube (CNT) is a graphite sheet rolled up into cylindrical shape with a nanoscale diameter. The major types of carbon nanotube are single-walled CNTs and multi-walled CNTs. Important properties of CNTs are high aspect ratio up to 3,300,000. It can be either metal or semiconductor depending on graphite roll up direction and it has high current density up to 4×10^{9} A/cm^{2} [3]. For mechanical property, it has higher Young's modulus and higher tensile strength than steel [4]. From the excellent properties of CNT, CNT is an ideal material for use as tip in AFM. Figure 1 shows schematic view of CNT-modified cantilever.

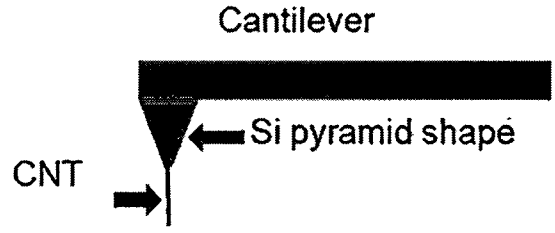

Figure 1 Schematic view of CNT-modified cantilever.

This material is reserved for educational use only, not allowed for commercial use.
Forbidden to modify the content, and cite the document when use.

To fabricate CNT cantilever, CNT is attached to the Si pyramid shape (conventional tip) of cantilever by three main methods; (1) using acrylic adhesive [5], (2) manipulation in scanning electron microscopy [6-7] and (3) direct growth of CNT on the Si pyramid shape by chemical vapor deposition (CVD) [8-11]. Direct growth gives a good mechanical contact between CNT and Si cantilever because Van der Waals forces between each CNT and the Si tip might play an important role in holding the CNT in place and maintaining its orientation. CNTs possess mechanical robustness because of its rooted growth from the network [14]. However acrylic adhesive method is easy but not good contact.

In Hard Disk Drive factory, AFM is the important tool for scan slider and media surface analysis. A lot of used cantilevers are used for characterization. So it is necessary to modify used AFM cantilever for imaging improvement and reduce the expense of the company. In this study, the used cantilever was used as a platform for CNT attachment by direct growth method of Ni catalyst-assisted CVD using ethanol as carbon source.

1.2 Objectives

1.2.1. To establish a method to attach CNTs on the used AFM cantilever.

1.2.2. To establish a method for metal catalyst thin film deposition on the pyramid shape of cantilever.

1.2.3. To establish the optimal conditions of chemical vapor deposition (CVD) for direct growth of CNT on used AFM cantilever.

1.2.4. To investigate the imaging performance of the modified used-AFM cantilevers by attachment of CNTs on the apex.

This material is reserved for educational use only, not allowed for commercial use.
Forbidden to modify the content, and cite the document when use.

1.3 Scope of Research

1.3.1. Design AFM cantilever fixture to fix cantilever during electroplating process.

1.3.2. Investigate optimal conditions and Ni electroplating on pyramid shape of cantilever.

1.3.3. Investigate optimal conditions of CVD for direct growth of CNT on used AFM cantilever.

1.3.4. Characterize the morphology and structure of the synthesized CNT by field emission scanning electron microscopy (FESEM), high resolution transmission electron microscopy (HRTEM) and Raman spectrometer.

1.3.5. Investigate AFM imaging performance of the CNT-modified AFM cantilever and compare with those of new and used AFM cantilevers.

1.4 Expected Results

1.4.1. Establish the method to deposit metal catalyst thin film on the pyramid shape of used AFM cantilever.

1.4.2. Establish the method to attach CNTs on the used AFM cantilever.

1.4.3. Improve the imaging performance of used AFM cantilevers by modification with CNT on tip apex.

1.4.4. Reduce the expense of the company and high resolution AFM cantilever.

This material is reserved for educational use only, not allowed for commercial use.
Forbidden to modify the content, and cite the document when use.

Chapter 2
LITERATURE REVIEW

This chapter is a summary of the critical points of current researches on fabrication of carbon nanotubes (CNTs) for AFM tip and W tip application, and preparation of Ni thin film by electroplating technique for CNTs growth.

E. Yenilmez *et al.* improved fabrication of carbon nanotube for AFM tip in mass production by wafer scale production technique [12]. The method for CNTs synthesis was catalyst-assisted chemical vapor deposition (CVD) method. Their method reproducibility leads to the growth of single-walled CNTs (SWNTs) extending from Si tips on the wafer more than 90%, thus accomplishing a major task for mass production of nanotube probe tips. The catalyst-patterning step is accomplished by placing a catalyst onto 375 prefabricated Si tips by a simple technique that involves photoresist spin coating, catalyst deposition, and liftoff. For CVD, methane was used as the carbon feedstock. CVD system was heated to 900°C in an Ar flow. Ultrahigh purity methane 99.99% (flow rate of 1500 sccm) mixed with hydrogen (flow rate of 125 sccm) were switched into the CVD system for a growth time of 7 min, followed by cooling of the system to room temperature in a H_2 flow. The schematic view of the process is shown in Figure 2.1.

This material is reserved for educational use only, not allowed for commercial use.
Forbidden to modify the content, and cite the document when use.

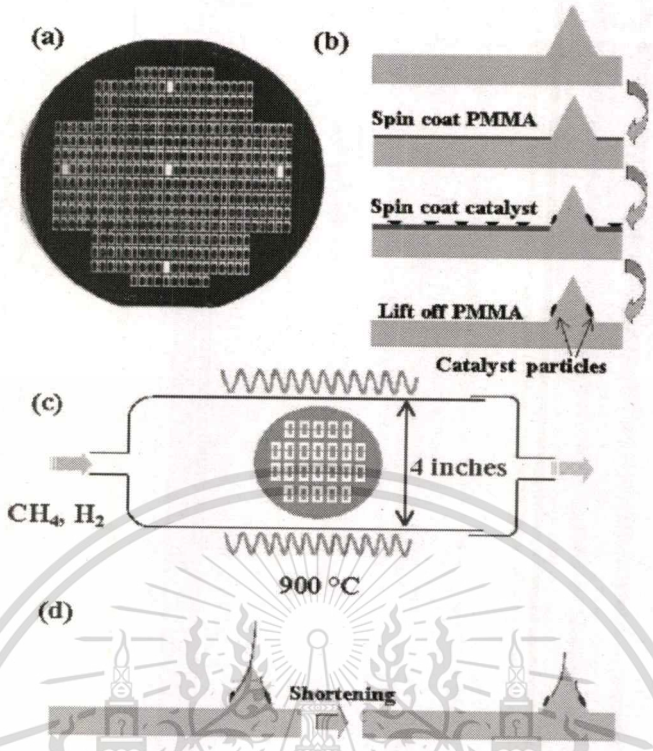

Figure 2.1 (a) Photograph of a 4 inch wafer containing 375 AFM cantilevers with integrated Si tips (photo courtesy of D. Adderton, Nanodevices Inc). (b) Schematic process flow for placing catalyst onto Si tips on a wafer. (c) CVD setup for growth on a wafer. (d) Long nanotubes extending out of the Si tips are shortened [12].

TEM reveals that the structures extending outward from the Si tips consist of either individual SWNTs (2 nm in diameter) or bundles of SWNTs with diameters up to 10 nm. Van der Waals forces between the nanotubes and the pyramids are responsible for holding the nanotubes in place. The SWNTs grown from the Si pyramids typically extend outward from the tips 1–10 μm. These nanotubes are shortened to about 30–100 nm to obtain mechanically rigid nanotube probe tips for AFM operation by etching from oxygen discharge. Figure 2.2 shows SEM and TEM images of as-grown nanotube tips.

Even though, this process can produce CNT-AFM tip for mass production but preparing of catalyst on the Si tip by lithography was quite complicated and high cost of budget. Furthermore, the resultant of CNT length is too long, thus step of shortening CNTs on AFM tip is required.

This material is reserved for educational use only, not allowed for commercial use.
Forbidden to modify the content, and cite the document when use.

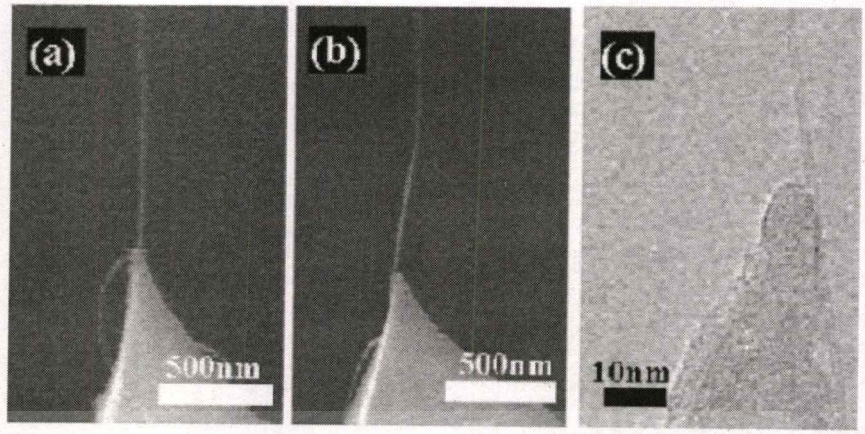

Figure 2.2 (a), (b) SEM images of as-grown nanotube tips. 10 nm of Ti was evaporated onto the samples for SEM imaging. (c) TEM image of a SWNT extending from a Si tip [12].

K. Takagahara *et al.* has developed the technique to increase the yield of CNTs at the apex of AFM probes [13]. CNTs were synthesized at the apex of the commercial AFM tips by CVD process with applying an electric field. The yield of AFM probes with CNTs at the apex increased approximately 52%. A voltage of 40 V was applied between a titanium jig and a silicon counter electrode. The gap between the probe apex and the counter electrode was 60 μm. The AFM probes have electrical contact with the jig. An electric field produced by the voltage concentrates at the probe tips because their apexes are very sharp. Thermal oxidation was carried to form a glass (SiO_2) layer on the AFM probes because catalysts for the CVD process were fixed only on the SiO_2 surface. Fe and Co were used as catalytic metals for the CVD process. Fe and Co acetate was dissolved in ethanol to form a metal acetate solution, both metals were prepared equally at 0.01 wt%. A catalyst layer was formed on the surface of the AFM probes by dip-coating for 10 min. After catalyst coating, the probes were dried in a 400°C of oven to remove organic residues and to form oxidized bimetallic particles on the SiO_2 surface. Then, SiO_2 layer was partially removed by HF to make an electrical connect with the jig. For CVD process, the quartz tube was heated up to 800°C under atmosphere of Ar/H_2 (3% of H_2 gas) gas at a flow rate of 300 sccm at a pressure of 40 kPa. When the temperature reached to 800°C, the Ar/H_2 gas was stopped and the quartz tube was evacuated with a vacuum pump. A voltage of 40 V was applied between the probes and the counter electrodes by a voltage controller. Then ethanol vapor was introduced into the

This material is reserved for educational use only, not allowed for commercial use.
Forbidden to modify the content, and cite the document when use.

quartz tube, keeping the ethanol pressure at about 1.4 kPa for 25 min. The schematic view of the process is shown in Figure 2.3. The synthesized CNTs had 5-15 nm diameters and 300-5000 nm lengths. The CNT-AFM probes showed higher horizontal resolution than the standard commercial AFM probes. Figure 2.4 shows SEM images of side views of the AFM probes and close-up views of the tips after the CVD process.

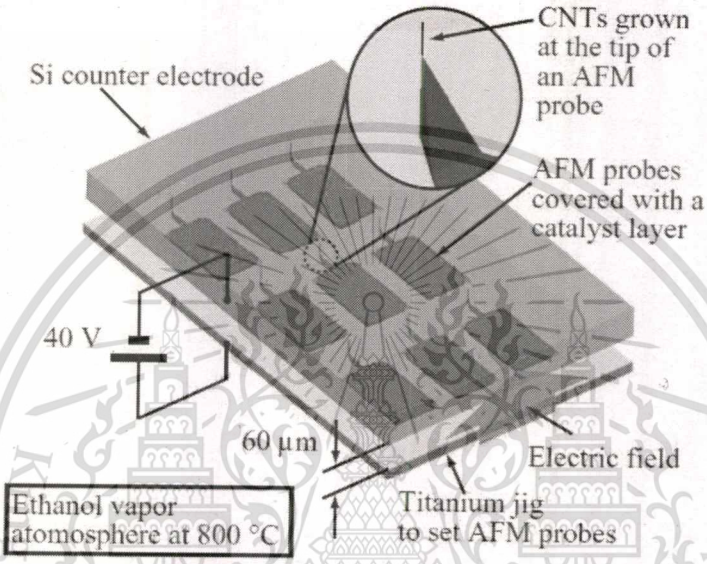

Figure 2.3 Schematic diagram of batch fabrication of CNTs at the tips of AFM probes [13].

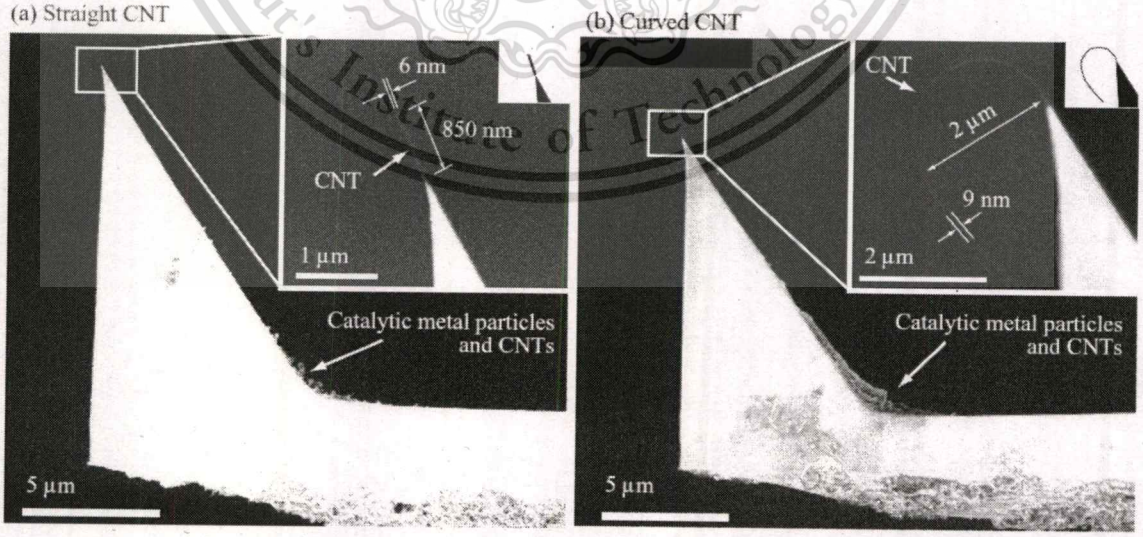

Figure 2.4 SEM images of side views of the AFM probes and close-up views of the tips after the CVD process. (a) A probe tip with a straight CNT (b) A probe tip with a curved CNT [13].

This material is reserved for educational use only, not allowed for commercial use.
Forbidden to modify the content, and cite the document when use.

The key point of this paper is the design of jig in order to hold wafer of AFM tip. Each probe tip has the same distance to the counter electrode and the probe tip is protected from mishandling of load – unload to the quartz tube of CVD process. However, CVD process of this paper was quite complicated and it also need vacuum system. Moreover dip coating for metal catalyst in this paper give abundance of CNTs on the cantilever as shown in Fig. 2.4.

W. Wongwiriyapan *et al.* successfully synthesized SWNTs protruding from the W tip apex and this process is reproducible [14]. An electrochemically etched W tip with a diameter of 0.25 mm and a curvature radius of approximately 100 nm [Fig. 2.5(a)] was used for SWNT growth. Prior to thermal CVD growth, Fe (0.5 – 2 nm) catalytic thin films with a support layer of Al (5 – 10 nm) were deposited on the W tip by E-beam evaporation at room temperature. The W tip was laid parallel to the gas flow direction. To form catalyst nanoparticles, the tip was annealed in a quartz tube at 850°C for 30 min under a flow of Ar gas at a flow rate of 300 sccm. Then, Ar gas was replaced with pure CH_4 (99.99%) as a source gas with a pressure of 53 kPa at a flow rate of 300 sccm. The CVD growth of CNTs was carried out at 850°C for 5 min. Figures 2.5(b)–(d) show SEM images of the resultant SWNTs at the optimal catalyst thickness; Fe (2 nm)/Al (10 nm). Figure 2.5(b) shows SEM image of the SWNTs grown on region A of Figure 2.5(a) where the circumference of the tip was approximately 5 mm. A high-yield growth of SWNT networks with an approximately uniform diameter was observed. The density of the SWNT networks gradually decreased with proximity to the W tip apex as shown in Figure 2.5(c). The SWNTs that protruded from the W tip apex were relatively straight with diameters ranged from 0.9 to 3.7 nm and lengths from 200 nm to 1 mm. The Raman spectrometer data also gave evidence of the growth of SWNTs. The sharp and branched peak of the G band (at approximately 1590 cm^{-1}) with a very small D band (at approximately 1350 cm^{-1}) and the radial breathing mode (at approximately 150 – 280 cm^{-1}) implied the high-yield production of SWNTs on the W tip.

This material is reserved for educational use only, not allowed for commercial use.
Forbidden to modify the content, and cite the document when use.

The key point of this report is the effective role of the Al layer was attributed to the high-yield growth of SWNTs. The Al layer transformed into Al oxide clusters, it acting as a catalyst support. It is likely that the Al layer also acts as a reaction barrier against the formation of Fe–W alloy, resulting in the activation of the Fe catalyst. The drawback is preparing of Fe/Al catalytic thin films by electron-beam evaporation was quite complicated.

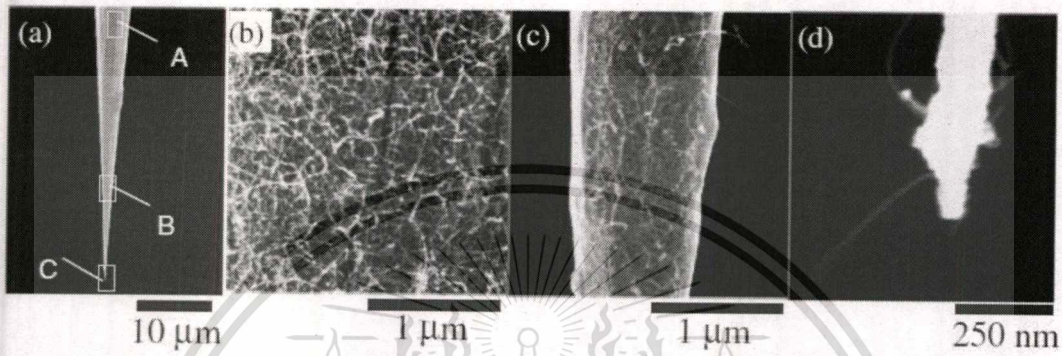

Figure 2.5 (a) SEM image of W tip before thermal CVD growth. (b)–(d) SEM images of W tip after thermal CVD growth in regions A, B, and C in (a), respectively [14].

C. S. Han *et al.* reported the fabrication and characterization of CNT tip modified by focused ion beam (FIB) [15]. First, dielectrophoresis method was used for CNT attachment on AFM probes due to its easy experimental setup, low cost, and a high success rate. For the excellent imaging capability, CNT-AFM tip should satisfy suitable length and vertical angle to the substrate, otherwise, imaging quality would be degraded. To make the high performance CNT-AFM tip, FIB technique was used to align the attachment angle and to cut the length of the CNT. In this paper, it was focused on the performance evaluation of the FIB-modified tip in terms of wear, image resolution and trench structure. FIB-modified CNT tip showed better characteristics than normal Si tip. Figure 2.6 shows AFM results of AAO nano structures along with the scanning area. However, for practical application, FIB machine is highly expensive and complicated using.

This material is reserved for educational use only, not allowed for commercial use.
Forbidden to modify the content, and cite the document when use.

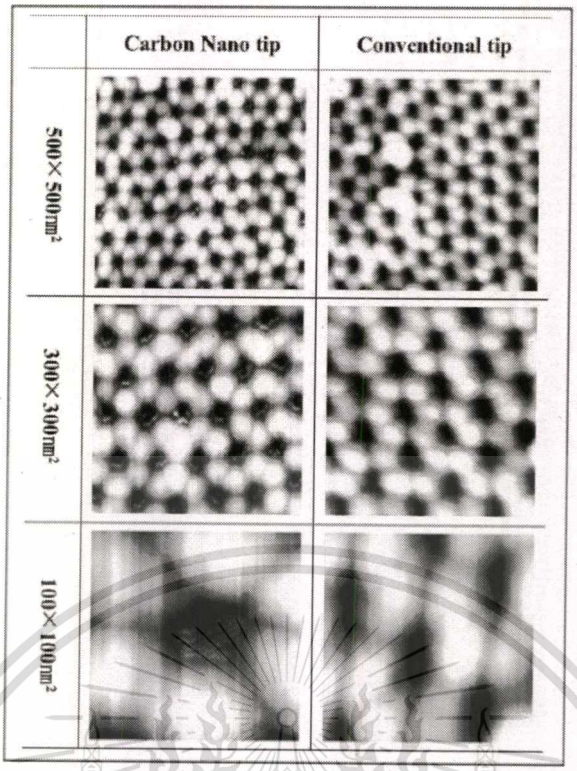

Figure 2.6 AFM results of AAO Nano Structures along with the scanning area [15].

J. Kim *et al.* demonstrated growth and field emission of carbon nanotubes on electroplated Ni catalyst coated on glass substrate [16]. The Ni catalyst was prepared by electroplating method. CNTs were synthesized from Ni catalyst coated on soda-lime glass substrates using CVD of C_2H_2 gas at 550°C. A 25x25 mm sized soda-lime glass was used as a substrate. Ag film, which is used as a cathode electrode, was printed by the screen - printing method of Ag paste DS - 7068. The printed pattern was a stripe type, 500 mm wide with 500 mm pitch. After printing the Ag film, it was dried at 150°C for 10 min and heated at 550°C for 10 min. The final thickness of the Ag film was about 5 mm on the glass substrate. The 200 nm thick Ni film was only coated on the patterned Ag film as a stripe line using the electroplating method to produce self-aligned CNTs grow on the line patterned Ni/Ag film. The electroplating bath consists of nickel sulfate ($NiSO_46H_2O$) 150 g/l, ammonium chloride (NH_4Cl) 15 g/l, and boric acid (H_3BO_3) 15 g/l. The temperature and pH of the electroplating bath were 40°C and 4.5, respectively. In the electroplating bath, an anode (+) of dc power source HC - 1330A was connected to a Ni metal plate and a cathode (-) was

This material is reserved for educational use only, not allowed for commercial use.
Forbidden to modify the content, and cite the document when use.

connected to the Ag coated glass substrate. The dc current ; 20 mA at 2 V was applied for 20 s. Figure 2.7 shows SEM micrographs of the CNTs grown on the Ni/Ag/glass substrate at 550°C using C_2H_2 gas with a flow rate of 20 sccm for 10 min. Raman spectrum reveals that CNTs have a defective graphite structure at the wall.

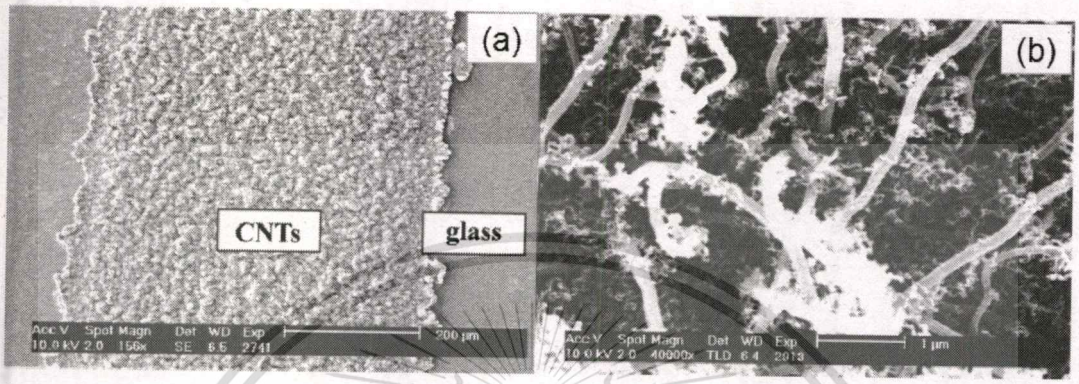

Figure 2.7 SEM micrographs of the CNTs grown on the Ni/Ag/glass substrate at 550°C using C_2H_2 gas with a flow rate of 20 sccm for 10 min, in the presence of a Pd gas activator. (a) SEM image of CNTs on the substrate. CNTs are selectively grown on the Ni catalytic metals. (b) A magnified SEM image (40000x) of CNTs [16].

M. K. Singh *et al.* showed the technique to synthesize high density of CNTs on Cu substrate by microwave plasma chemical vapor deposition (MPCVD) using electroplated Ni as catalyst [17]. Thin Cu foil was used as the substrate for the nanotube deposition. The foils have polycrystalline nature and have commercial grade purity (98%) without any special pre-treatment to improve their smoothness. The electroplating of the Ni coatings on Cu foils was performed in an electroplating bath. The Cu foil was used as cathode and a thin platinum wire was used as anode. Commercial grade nickel sulfate ($NiSO_47H_2O$); nickel chloride ($NiCl_26H_2O$) and boric acid (H_3BO_3) were used as electrolytes in a dc electroplating process. The bath temperature was maintained at 60°C and its pH was 3.5. The Ni layers having a thickness 15 μm were treated in plasma of NH_3 gas for 2 min prior to the deposition of CNTs in MPCVD apparatus. The temperature of the NH_3 treatment was 800 ± 20 °C and its flow rate was 180 sccm at a pressure of 20 mbar. CH_4 and H_2 were used as the precursor gases and their flow rates were 6 and 20 sccm, respectively. The substrate temperature during the nanotubes growth was 840 ± 20°C. Figure 2.8

This material is reserved for educational use only, not allowed for commercial use.
Forbidden to modify the content, and cite the document when use.

shows SEM image of the tubes on Cu substrate. The synthesized CNTs have length of 40-50 μm and inner diameter in the range 20-50 nm.

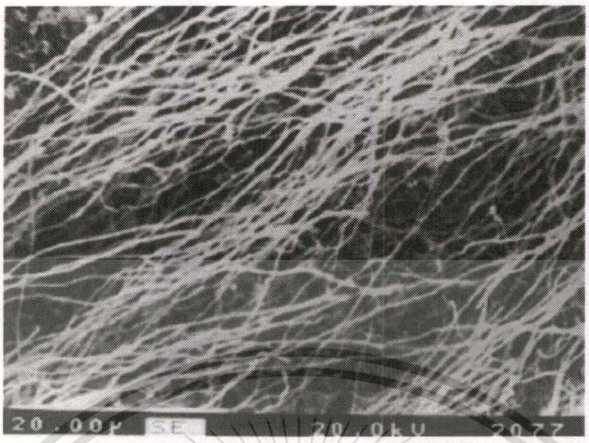

Figure 2.8 SEM image showing the morphology of the tubes on Cu substrate. The exceptionally long CNTs nearly parallel to the substrate are noteworthy [17].

There are many research papers regarding growth of CNTs on Si AFM probe tips. However, all of them were demonstrated by using the new commercial Si AFM cantilever as a platform. In this study, the used cantilever was demonstrated to be reused by CNT attachment by direct growth method of Ni catalyst assisted CVD using ethanol as carbon source.

To synthesize CNT by CVD method, metal catalyst must be formed prior CVD process. For metal catalyst preparation, sputtering or e-beam evaporation were adopted. These techniques require vacuum system and expensive. Although, dip-coating is a simple method but it is hard to control area of catalyst on AFM cantilever. It occasionally need to have cover layer (mask) to protect the unwanted of coating area. In this study, Ni electroplating method was chosen for metal catalyst because it is simple and metal catalyst can selectively attach at the tips easily due to the high density of electric field at the tip apex according to its sharpness. For CVD process, growth of the CNT on AFM tip can carry out without vacuum system but it is necessary to investigate the optimal condition such as electrode distance variation, plating time of catalyst formation, flow rate of ethanol during CVD process, CVD temperature and sample position in the quartz tube.

This material is reserved for educational use only, not allowed for commercial use.
Forbidden to modify the content, and cite the document when use.

CHAPTER 3

THEORY

3.1 Atomic Force Microscopy (AFM)

3.1.1 Principle

The principle of operation of the AFM is a sharp cantilever tip interacts with the sample surface sensing the local forces between the molecules of the tip and sample surface. The most characteristic property of the AFM is that the images are acquired by measuring the sample surface without using light. In this way, not only the sample topography can be recorded with good resolution, but also the material characteristics and the strength of interaction between the sample surface and the cantilever tip. Due to the fact that no light is involved in acquiring the sample properties, the AFM reaches a resolution far below the diffraction limit offered by the optical microscopy. Its resolution is limited only by the tip radius and the spring constant of the cantilever [18]. Figure 3.1 shows schematic diagram of AFM.

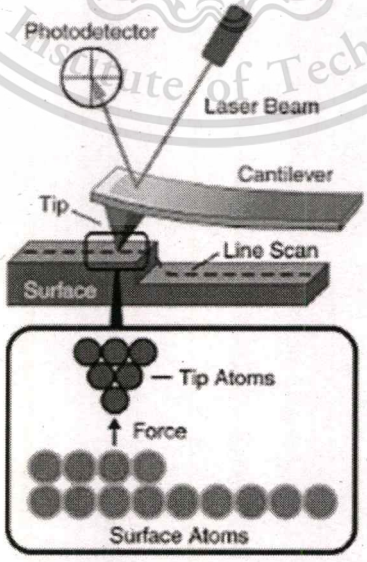

Figure 3.1 Schematic diagram of AFM [19].

This material is reserved for educational use only, not allowed for commercial use.
Forbidden to modify the content, and cite the document when use.

3.1.2 Mode of AFM Operation

Atomic Force is potential changes depending on the distance between two atoms. Figure 3.2 shows Lennard Jones Potential, relation between atomic force and distance.

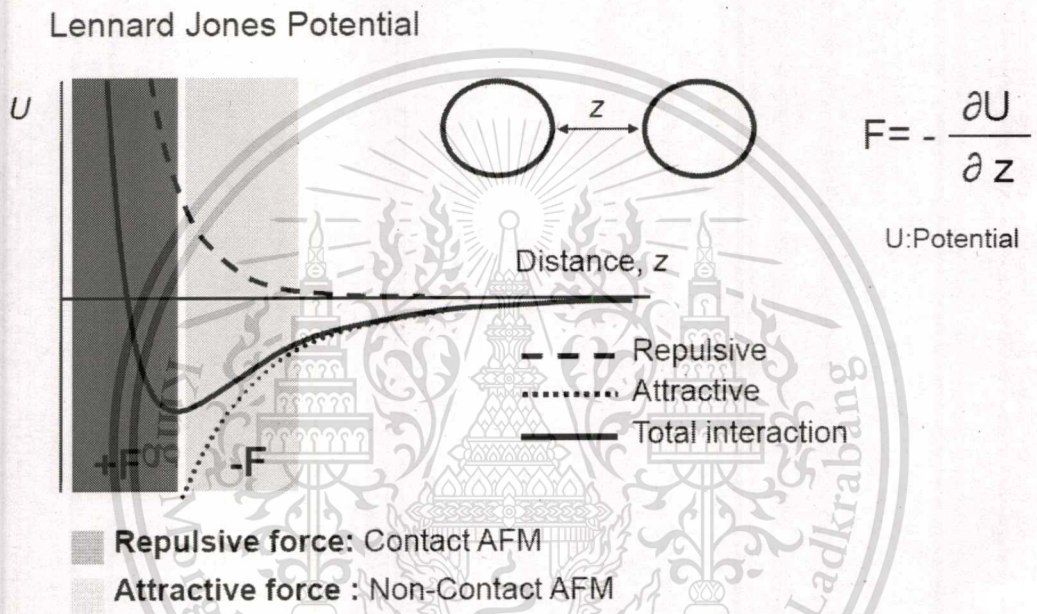

Figure 3.2 Lennard Jones Potential [20].

3.1.2.1 Contact mode

In the static mode operation, the static tip deflection is used as a feedback signal. Because the measurement of a static signal is prone to noise and drift, low stiffness cantilevers are used to boost the deflection signal. However, close to the surface of the sample, attractive forces can be quite strong, causing the tip to "snap-in" to the surface. Thus static mode AFM is almost always done in contact where the overall force is repulsive. Consequently, this technique is typically called "contact mode". In contact mode, the force between the tip and the surface is kept constant during scanning by maintaining a constant deflection.

This material is reserved for educational use only, not allowed for commercial use.
Forbidden to modify the content, and cite the document when use.

3.1.2.2 Tapping mode

In ambient conditions, most samples develop a liquid meniscus layer. Because of this, keeping the probe tip close enough to the sample for short-range forces to become detectable while preventing the tip from sticking to the surface presents a major problem for non-contact dynamic mode in ambient conditions. Dynamic contact mode (also called intermittent contact, AC mode or tapping mode) was developed to bypass this problem [21]. In tapping mode, the cantilever is driven to oscillate up and down at near its resonance frequency by a small piezoelectric element mounted in the AFM tip holder similar to non-contact mode. A tapping AFM image is therefore produced by imaging the force of the intermittent contacts of the tip with the sample surface [22].

3.1.2.3 Non-contact mode

In this mode, the tip of the cantilever does not contact the sample surface. The cantilever is instead oscillated at either its resonant frequency. The van der Waals forces, which are strongest from 1 nm to 10 nm above the surface, or any other long range force which extends above the surface acts to decrease the resonance frequency of the cantilever. This decrease in resonant frequency combined with the feedback loop system maintains a constant oscillation amplitude or frequency by adjusting the average tip-to-sample distance. Measuring the tip-to-sample distance at each (x,y) data point allows the scanning software to construct a topographic image of the sample surface [23]. Equation 3.1 and 3.2 show finding of frequency of vibration and simple harmonic oscillator, respectively [20].

$$k_{eff} = k_0 - \frac{\partial f}{\partial r} \qquad (3.1)$$

where

k_0 : Intrinsic spring constant

k_{eff} : Effective spring constant

This material is reserved for educational use only, not allowed for commercial use.
Forbidden to modify the content, and cite the document when use.

$$\omega = \sqrt{\frac{k_{eff}}{m}} \tag{3.2}$$

3.1.3 Imaging Resolution

Figures 3.3 and 3.4 show effect of tip sharpness on imaging resolution. For sharp tip, image resolution depends on haft-cone angle as shown in Fig. 3.3. However for dull tip, image resolution depends on tip size and has the different geometry from the sample as shown in Fig. 3.4

Sharp tip, r < R

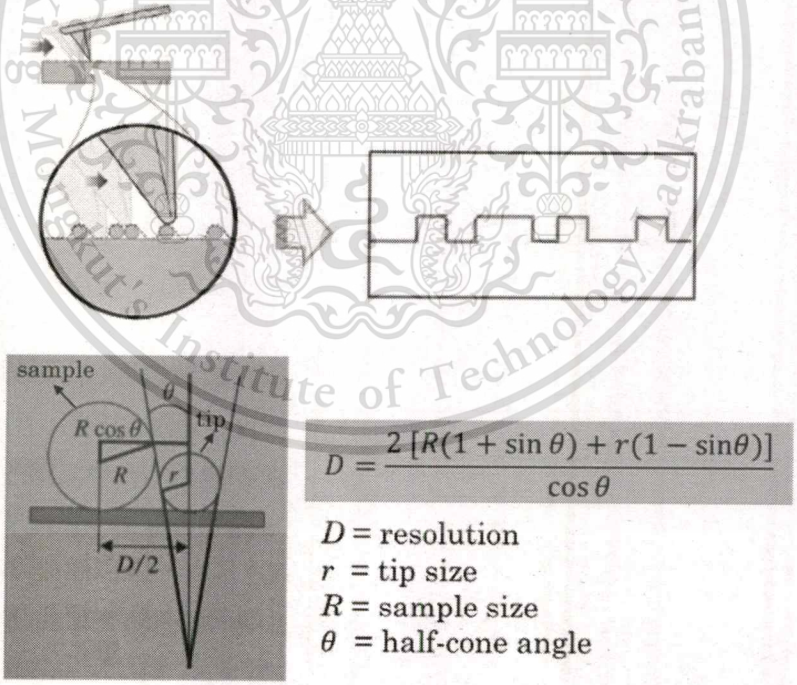

Figure 3.3 Effect of sharp tip on imaging resolution [20, 24].

This material is reserved for educational use only, not allowed for commercial use.
Forbidden to modify the content, and cite the document when use.

Dull tip, r > R

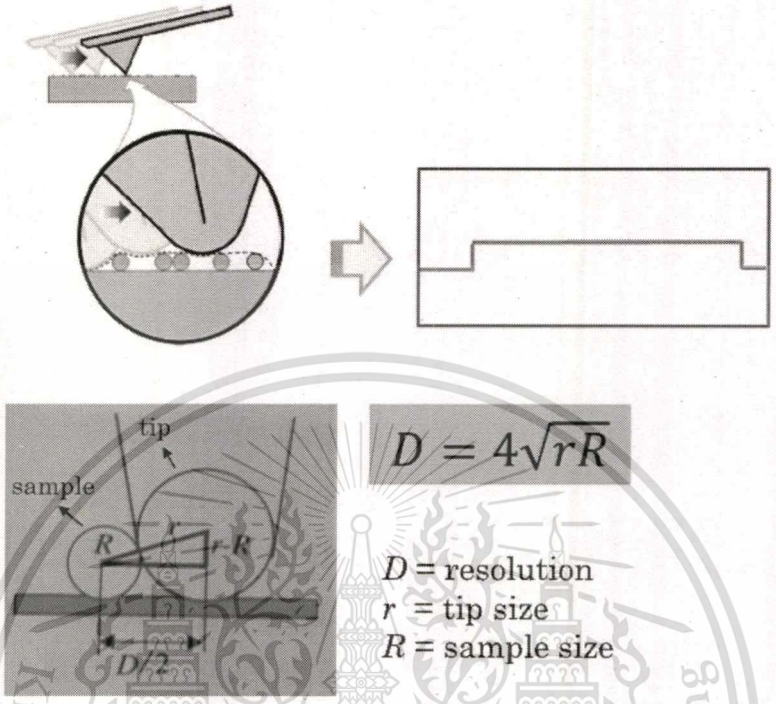

Figure 3.4 Effect of dull tip on imaging resolution [20, 24].

3.2 Carbon Nanotubes

3.2.1 Types of CNTs

There are two basic types of CNTs: single-wall carbon nanotubes (SWCNTs) which are the fundamental cylindrical structure and multi-wall carbon nanotubes (MWCNTs) which are made of coaxial cylinders having interlayer spacing close to that of the interlayer distance in graphite (0.34 nm). These cylindrical structures are only few nanometers in diameter, but the cylinder can be tens of microns long, with most end capped with half of a fullerene molecule. It was first discovered by M. Endo in 1978, as part of his Ph.D. work at the University of Orleans in France, but real interest in CNTs started when Iijima (1991) first reported it in 1991 [25]. Figure 3.5 shows schematic diagrams of SWCNT and MWCNT.

This material is reserved for educational use only, not allowed for commercial use.

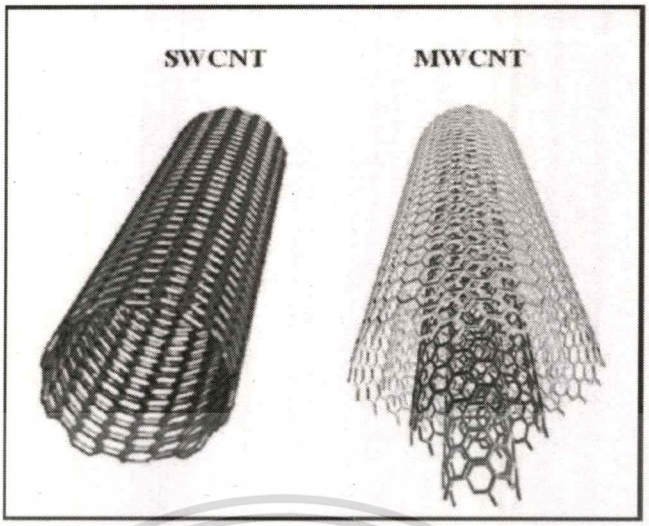

Figure 3.5 Schematic diagrams of SWCNT and MWCNT [25].

3.2.2 Synthesis of CNTs

3.2.2.1 Arc discharge

The carbon arc discharge method, initially used for producing C_{60} fullerenes, is the most common and perhaps easiest way to produce CNTs. But this technique produces graphitic impurities such as carbon soot containing amorphous carbon, anions and fullerenes. In this method an inert gas atmosphere is created in the reaction vessel by passing an inert gas at controlled pressure. Two graphitic rods constitute the electrodes, between which a potential difference is applied. As the rods are brought closer, a discharge occurs, resulting in formation of plasma. The deposit, which contains CNTs, forms on the large negative electrode (cathode) while the smaller positive electrode (anode) is consumed. When a metal catalyst is used along with graphite, a hole is drilled in the carbon anode and it is filled with a mixture of metal and graphite powder. In this case, most nanotubes are found in soot deposited on the arc chamber wall [26]. Figure 3.6 shows schematics of plasma arc discharge.

This material is reserved for educational use only, not allowed for commercial use.
Forbidden to modify the content, and cite the document when use.

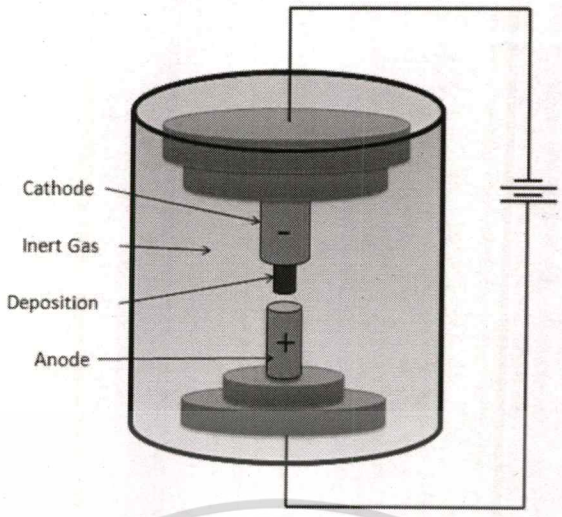

Figure 3.6 Schematics of plasma arc discharge [27].

3.2.2.2 Laser ablation

Laser ablation uses an intense laser pulse to vaporize a carbon target, which also contains small amount of metals such as nickel and cobalt and is placed in a tube furnace at 1200°C. As the target is ablated, inert gas is passed through the chamber carrying the grown nanotubes on a cold finger for collection. This method mainly produces SWCNT in the form of ropes [26]. Figure 3.7 shows schematics of laser ablation.

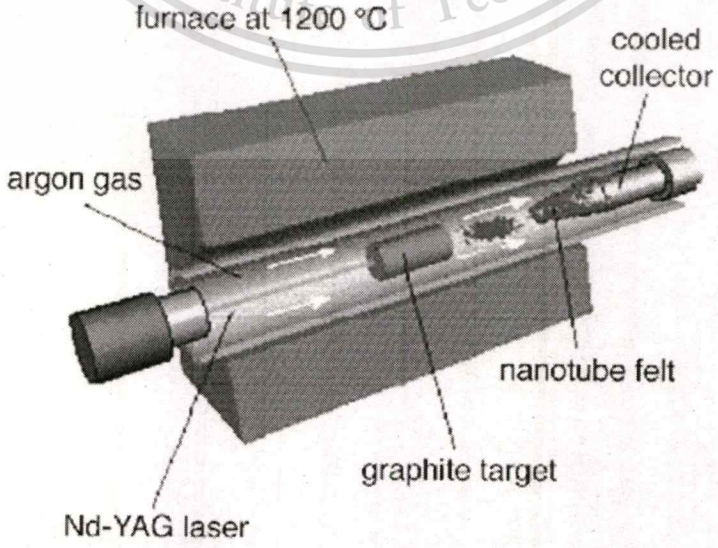

Figure 3.7 Schematics of laser ablation [27].

This material is reserved for educational use only, not allowed for commercial use.
Forbidden to modify the content, and cite the document when use.

3.2.2.3 Chemical vapor deposition

In this process a mixture of hydrocarbon, metal catalyst along with inert gas is introduced into the reaction chamber. During the reaction, nanotubes form on the substrate by the decomposition of hydrocarbon at temperatures 700–900°C and atmospheric pressure. The diameters of nanotubes that are to be grown are related to the size of the metal particles. This mechanism of CNT growth is still being studied. The first 'tip growth mode' where, the catalyst particles can stay at the tips of the growing nanotube during the growth process and second 'base growth mode' where, catalyst particles remain at the nanotube base, depending on the adhesion between the catalyst particle and the substrate. This technique offers more control over the length and structure of the produced nanotubes compared to arc and laser methods. This process can also be scaled up to produce industrial quantities of CNTs [26]. Figure 3.8 shows schematics of chemical vapor deposition oven. Figure 3.9 shows growth mechanisms for CNTs: (a) tip-growth model, (b) base-growth model.

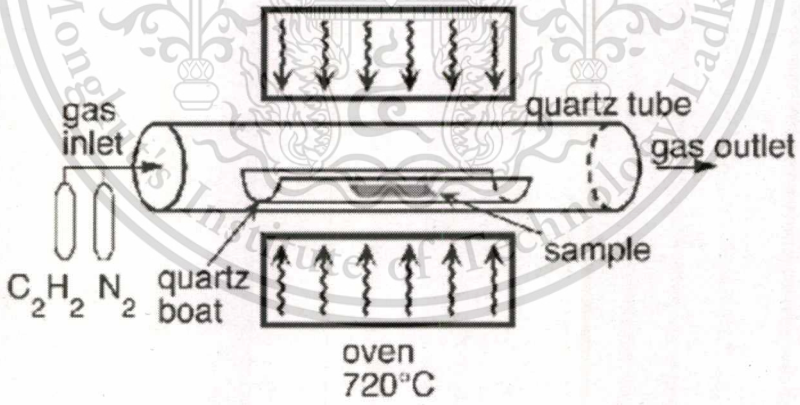

Figure 3.8 Schematics of chemical vapor deposition oven [27].

This material is reserved for educational use only, not allowed for commercial use.
Forbidden to modify the content, and cite the document when use.

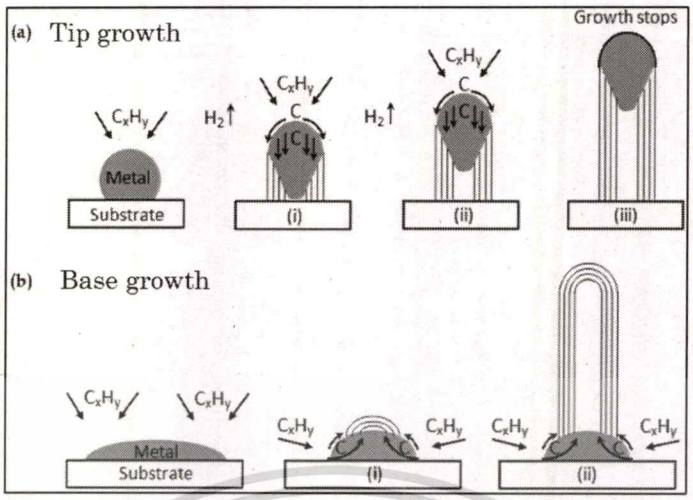

Figure 3.9 Growth mechanisms for CNTs: (a) tip-growth model, (b) base-growth model [26].

3.2.3 Properties of CNTs

Main properties of CNTs;

3.2.3.1 High aspect ratio (length/diameter)

It has a radius as small. Length is in the range from 200 nm - 1mm up and diameter is in the range from 3 Å - 200 nm. Aspect ratio is approximately 5,000 – 3,300,000.

3.2.3.2 Electrical properties

It can be either metal or semiconductor depending on graphite roll up direction and it has high current density. Highest current density is at 4×10^9 A/cm^2 [3]. Figure 3.10 shows a sheet of graphite rolled to show formation of different types of single walled carbon nanotube. Armchair is conductor. Zigzag are conductor and semiconductor. Chiral is semiconductor.

This material is reserved for educational use only, not allowed for commercial use.
Forbidden to modify the content, and cite the document when use.

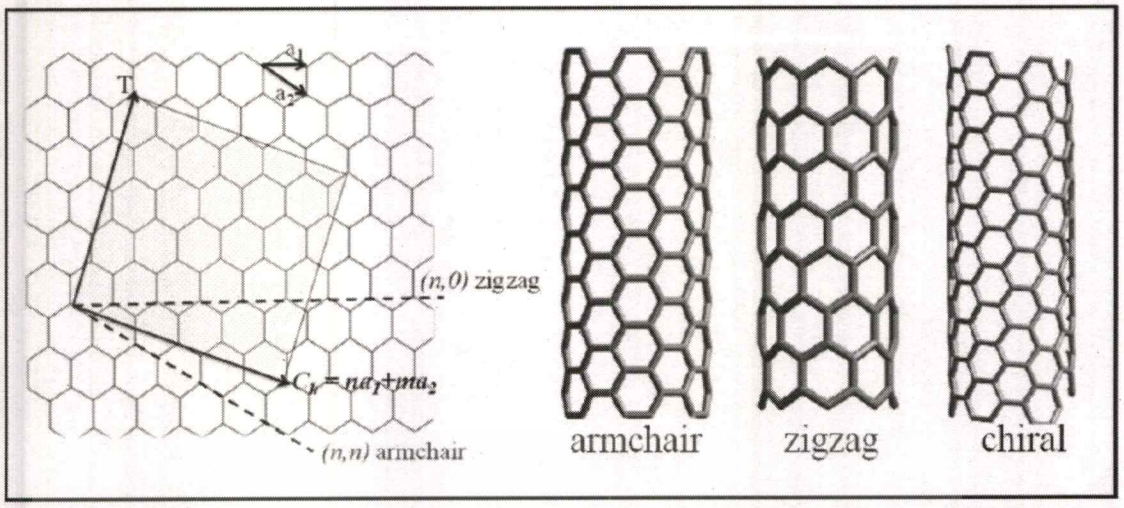

Figure 3.10 A sheet of graphite rolled to show formation of different types of single walled carbon nanotube [28].

3.2.3.3 Mechanical properties:

It has higher Young's modulus and higher tensile strength than steel. Table 3.1 shows mechanical properties of CNTs.

Table 3.1 Mechanical properties of CNTs [4].

	Young's modulus (Gpa)	Tensile Strength (Gpa)	Density (g/cm^3)
MWNT	1200	~150	2.6
SWNT	1054	75	1.3
SWNT bundle	563	~150	1.3
Graphite (in-plane)	350	2.5	2.6
Steel	208	0.4	7.8

This material is reserved for educational use only, not allowed for commercial use.
Forbidden to modify the content, and cite the document when use.

3.2.4 Applications of CNTs

With their excellent range of properties, CNTs have opened up a new age of advanced multifunctional materials. Incorporation of CNTs in polymer matrices provides materials that could be used for many high performance engineering applications. Currently, the most widespread use of CNT nanocomposites is in electronics. These nanocomposites could be used to shield electromagnetic interference and as electrostatic-discharge components. The microwave-absorbing capability of nanotubes could be exploited to heat temporary housing structures and may have applications in space exploration. Thin layers of nanotubes on plastics might also be used in transparent conducting composites. High mechanical strength of these nanocomposites could be utilized to make some high-end sporting goods such as tennis rackets, baseball bat etc, and thus delivering superior performance [26].

3.3 CNTs for AFM Cantilevers

Scanning probe microscopes, such as atomic force microscopes (AFM) and scanning tunneling microscopes (STM) are widely used now by the research community to image, characterize and manipulate surfaces, atoms and molecules and also by the semiconductor industry as a metrology tool. A serious problem in scanning probe microscope is the availability of tips having well-known structural and electrical properties as well as good mechanical and chemical stability. For example, a typical AFM probe consists of a silicon or silicon nitride cantilever with a pyramidal shaped tip. This tip can be made as small as 10-20 nm offering reasonable resolution. However, the large cone angle of this tip (30-35 deg.) makes it difficult for probing narrow and deep features. Another serious drawback is that the tip is brittle thus limiting its use in applications; either the tip breaks after only a limited use or becomes blunt.

This material is reserved for educational use only, not allowed for commercial use.
Forbidden to modify the content, and cite the document when use.

CNTs have nanometer scale diameter and high aspect ratio, are robust and stable under a wide range of applied physical conditions and can be functionalized. For these reasons, CNT tips have become an attractive alternative in scanning probe microscope. CNTs probes can be manually glued to the apex tip of an AFM cantilever suing acrylic adhesives or attached via electron beam deposition of amorphous carbon. Manipulation in scanning electron microscopy is one alternative. Alternatively, carbon nanotubes can be directly grown on the tips via CVD methods. In a well-characterized CVD process, it may be possible to control the length of the probe by selecting the growth time. On the other hand, it is possible to shorten a long tip to the desired length by the application of an electric field to etch away the carbon atoms.

AFM carbon nanotube tips prepared as above described, have demonstrated high resolution and superb stability with no damages for both tip and sample and consequent long lifetime, in imaging biological material, carbon nanotubes and deep sharp grooves, as well as in nanolithography patterning. The usefulness of carbon nanotubes as STM tips with atomic resolution has been demonstrated in air on chemically inactive surfaces [26].

There are three main methods for CNT- cantilever preparation. One method is acrylic adhesive technique, another one is SEM manipulation technique. Another one is direct growth by chemical vapor deposition or CVD. Direct growth method gives a good contact between CNT and cantilever. However acrylic adhesive method is easy but not good contact [12, 28, 29]. Figure 3.11 shows CNT-cantilever preparations. Figure 3.12 shows example of AFM imaging, gold nanoparticle.

This material is reserved for educational use only, not allowed for commercial use.
Forbidden to modify the content, and cite the document when use.

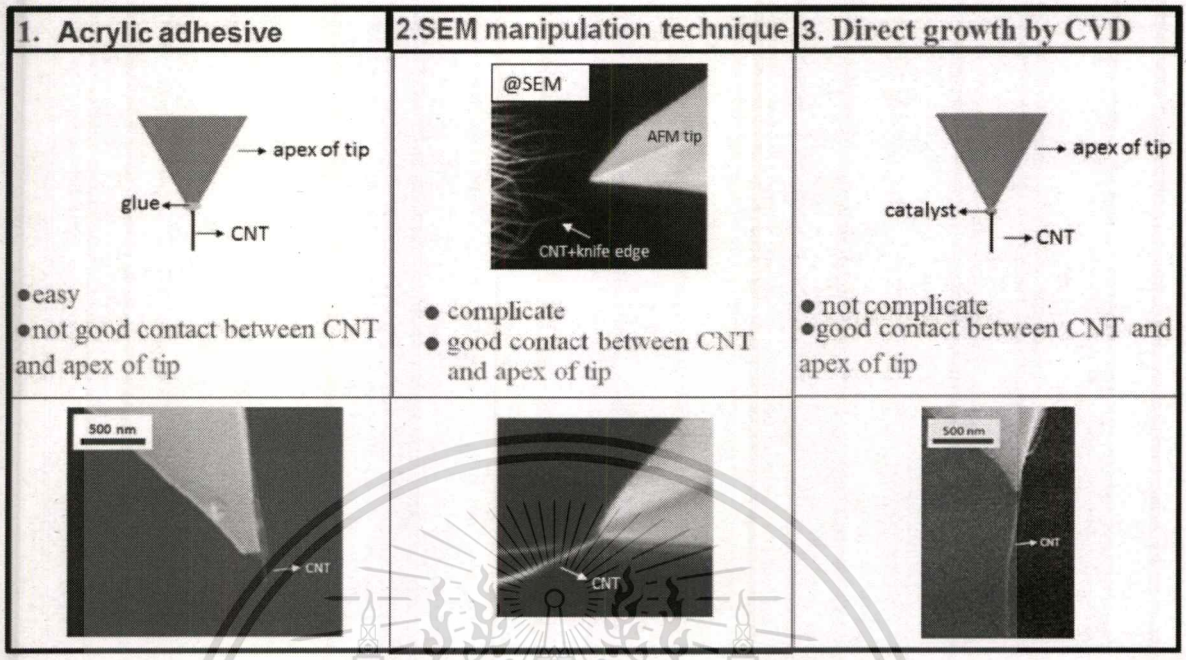

Figure 3.11 CNT-cantilever preparations [12, 28, 29].

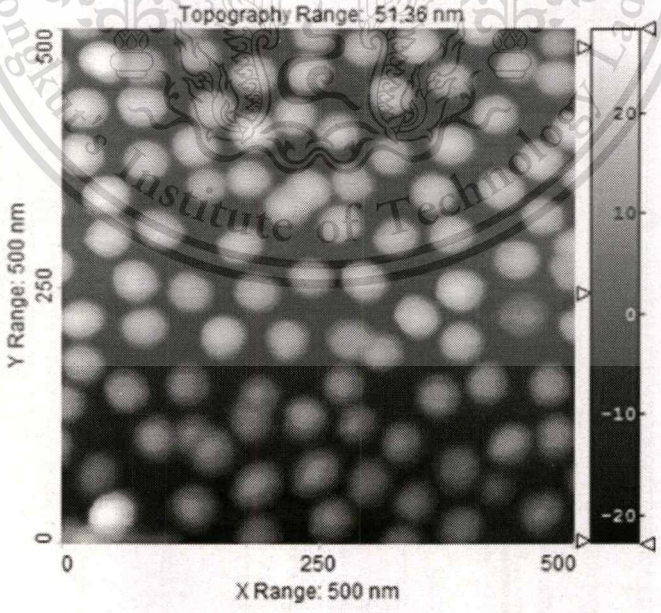

Figure 3.12 Example of AFM imaging, gold nanoparticle [30].

This material is reserved for educational use only, not allowed for commercial use.
Forbidden to modify the content, and cite the document when use.

3.4 Electroplating technique

Electroplating is the application of a metal coating to a metallic or other conducting surface by an electrochemical process. The article to be plated is set the cathode (negative electrode) of an electrolysis cell through which a direct electric current is passed. The article is immersed in an aqueous solution (the bath) containing the required metal in an oxidized form, either as cation or as a complex ion. The anode is usually a bar of the metal being plated. During electrolysis metal is deposited on to the work and metal from the bar dissolves [31]:

Cathode $Mz^{+}(aq) + ze^{-} \longrightarrow M(s)$

Anode $M(s) \longrightarrow Mz^{+}(aq) + ze^{-}$

3.4.1 Faraday's laws of electrolysis

Michael Faraday enunciated his laws of electrolysis in 1833. They are basic to both the understanding and the practical use of electrolytic processes. They may be stated as follows:

1. The amount of chemical change produced by an electrical current is proportional to the quantity of electricity that passes.

2. The amounts of different substances liberated by a given quantity of electricity are inversely proportional to their chemical equivalent weights.

3.4.2 Nickel Electroplating

To transfer nickel onto the surface of the article properly, a negative charge must be applied to the base material, while a rod made of nickel is connected to the positive side of the rectifier or power source [32].

Next, the article is submerged in a solution that features a salt with a chemical makeup, including the electroplating metal. For nickel electroplating, this solution

This material is reserved for educational use only, not allowed for commercial use.
Forbidden to modify the content, and cite the document when use.

consists of water and nickel chloride salt (or nickel sulfate salt). Due to the electric current present in the solution, the nickel chloride salt dissociates to negative chloride ions and positive nickel cations. The negative charge of the base metal then attracts the positive nickel ions, while the positive charge of the nickel rod attracts the negative chloride anions. Through this chemical reaction, the nickel in the rod oxidizes and dissolves into the solution. From here, the oxidized nickel is attracted to the article, and subsequently coats the article. The process of nickel electroplating is shown in figure 3.13.

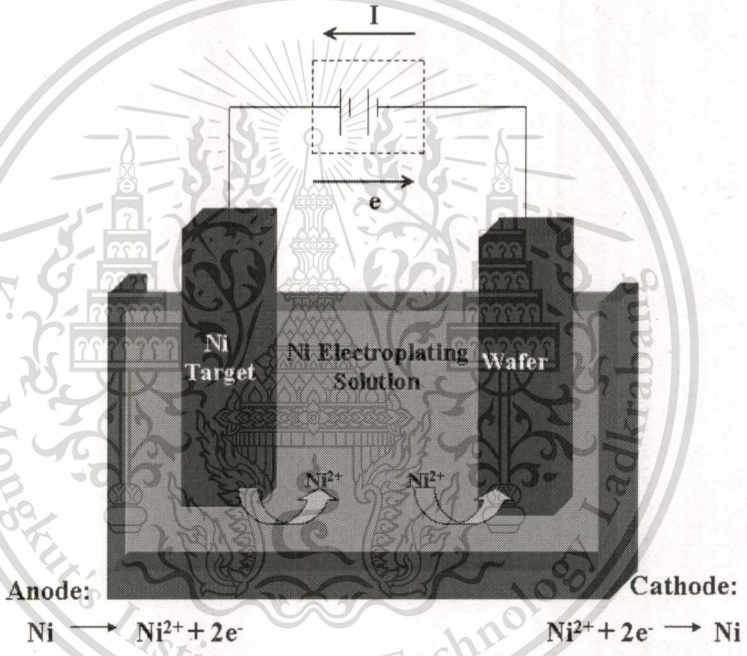

Figure 3.13 The process of nickel electroplating [33].

This material is reserved for educational use only, not allowed for commercial use.
Forbidden to modify the content, and cite the document when use.

3.4.3 Thickness of thin films

The thickness of thin films can calculate from Faraday's laws as showing below [34].

$$W = \frac{ItA}{nF} \qquad (3.5)$$

where

W = weight of plated metal in grams

I = current in coulombs per second

t = time in seconds

A = atomic weight of the metal in grams per mole

n = valence of the dissolved metal in solution in equivalents per mole

F = Faraday's constant in coulombs per equivalent (F = 96,485.309 coulombs/equivalent)

The following illustration will describe how Faraday's Law can be used. Consider nickel electroplating. The electrochemical reaction at the cathode will be:

$$Ni^{2+} + 2e^{-} = Ni \qquad (3.6)$$

This material is reserved for educational use only, not allowed for commercial use.
Forbidden to modify the content, and cite the document when use.

Equation 3.6 means that nickel ions in solution will plate out as nickel metal on the cathode when two electrons per nickel ion are passed into solution. The thickness of the electroplated metal can calculate this thickness using the following equation (3.7):

$$T = \frac{W \times 10000}{\rho \times S} \qquad (3.7)$$

where

T = thickness in microns

S = surface area of the plated part in square centimeters

ρ = density in grams per cubic centimeter

10000 = is a multiplicative constant to convert centimeters to microns

If equations (3.5) and (3.7) are combined we have the following equation for plated thickness in equation (3.8).

$$T = \frac{ItA \times 10000}{nF \times \rho \times S} \qquad (3.8)$$

This material is reserved for educational use only, not allowed for commercial use.
Forbidden to modify the content, and cite the document when use.

3.5 Analytical Methods

3.5.1 Field Emission Scanning Electron Microscopy: FESEM

FESEM is microscope that works with electrons instead of light. The field emission scanning electron microscope is a type of electron microscope that images the sample surface by scanning it with a high-energy beam of electrons in a raster scan pattern. The system uses a thermal field emission source to provide a stable high beam current. Detector of secondary electron is placed in the microscope that collect signal to produce an image of the specimen. It is mounted at the right hand side of the chamber over the sample [35]. Figure 3.14 shows schematic diagram of main unit of SEM.

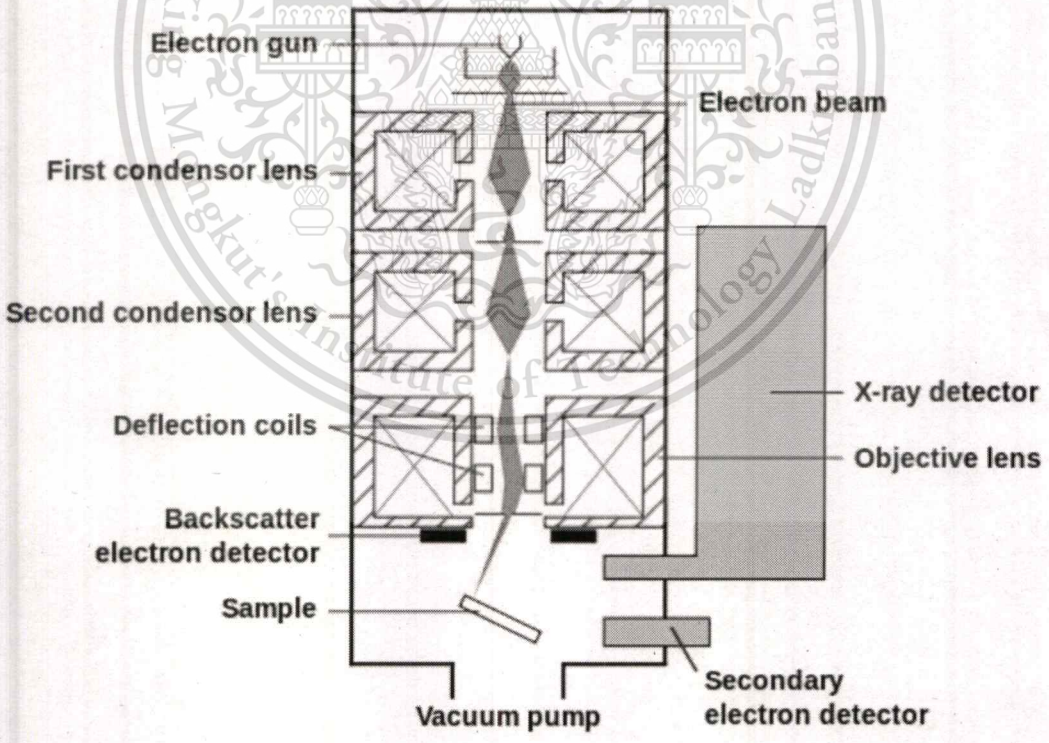

Figure 3.14 Schematic diagram of main unit of SEM [36].

This material is reserved for educational use only, not allowed for commercial use.
Forbidden to modify the content, and cite the document when use.

3.5.2 High Resolution Transmission Electron Microscopy: HRTEM

HRTEM is an instrument for high-magnification studies of materials sciences, nanotechnology, the semiconductor and data storage industries. High resolution makes it perfect for imaging materials on the atomic scale. High resolution transmission electron microscope use electron beam which occur from high voltage transmitted through filament. Electron depart from terminal of filament to object which electron beam raster to objective lens and signal was enlarged then electron will activate molecule of fluorescence screen in order to produce the 2D image. Dark-field image obtained from the object that have high atomic number while bright-field image obtained from the object that have low atomic number [37]. Figure 3.15 shows schematic diagram of main unit of TEM.

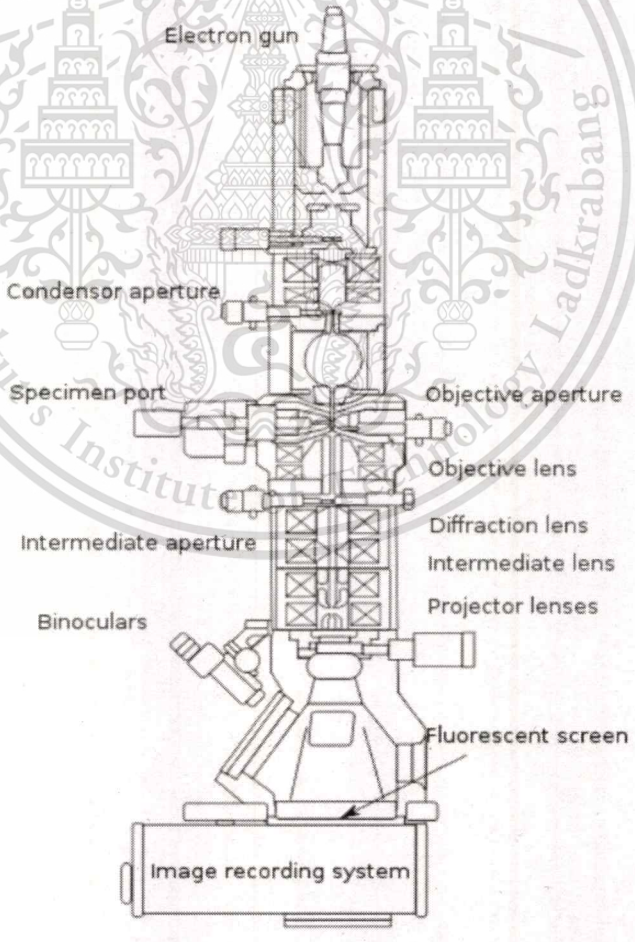

Figure 3.15 Schematic diagram of main unit of TEM [38].

This material is reserved for educational use only, not allowed for commercial use.
Forbidden to modify the content, and cite the document when use.

3.5.3 Raman spectrometer

Raman spectrometer is a spectroscopic technique based on inelastic scattering of monochromatic light, usually from a laser source. Inelastic scattering means that the frequency of photons in monochromatic light changes upon interaction with a sample. Photons of the laser light are absorbed by the sample and then reemitted. Frequency of the reemitted photons is shifted up or down in comparison with original monochromatic frequency, which is called the Raman effect. This shift provides information about vibrational, rotational and other low frequency transitions in molecules. Raman spectrometer can be used to study solid, liquid and gaseous samples [39]. Figure 3.16 shows Energy-level diagram. Energy-level diagram showing the states involved in Raman signal. The line thickness is roughly proportional to the signal strength from the different transitions.

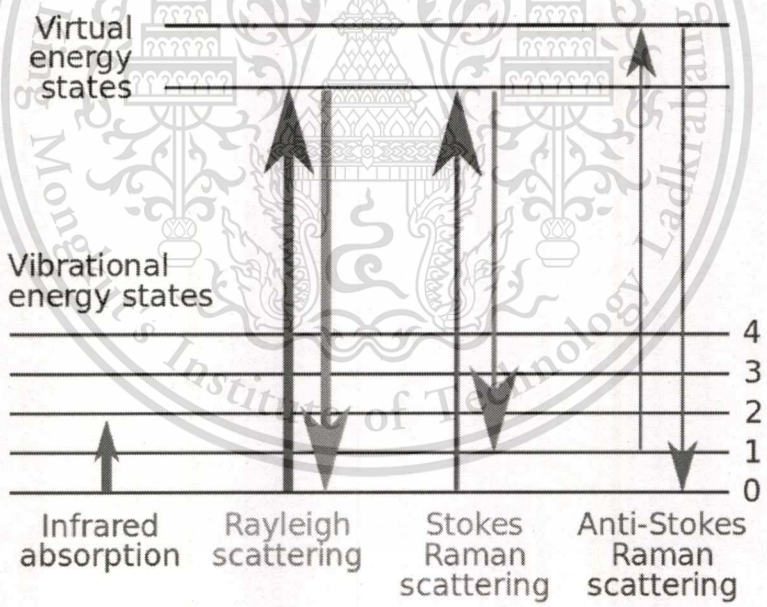

Figure 3.16 Energy-level diagram [39].

This material is reserved for educational use only, not allowed for commercial use.
Forbidden to modify the content, and cite the document when use.

CHAPTER 4

RESEARCH METHODOLOGY

This chapter describes steps of modification of used AFM cantilever by carbon nanotube (CNT) attachment. It consists of selection of used AFM cantilever for experiment, synthesis CNTs on AFM tip by floating Fe catalyst, synthesis CNTs on AFM tip by electroplated Ni catalyst, design of AFM cantilever fixture for electroplating, Ni deposition on used AFM cantilever by electroplating method, synthesis of CNTs on used AFM cantilever by chemical vapor deposition (CVD) method, CNT characterizations and AFM imaging performance test using CNT-modified AFM cantilever. Fabrication of CNT of this experiment divided into 2 methods. First method is synthesis CNTs on AFM tip by floating Fe catalyst. Second method is synthesis CNTs on AFM tip by electroplated Ni catalyst.

4.1 Selection of used AFM cantilever for experiment

The used AFM cantilever was observed by field emission scanning electron microscope (FESEM) before CNT attachment experiment. If used AFM tips were broken or had contaminations, those tips were not selected for the CNT attachment experiment. The used AFM cantilevers that are appropriate for the experiment should have curvature radius approximately 60 - 150 nm. If broken used tip is used for scanning, the AFM imaging will not be clear and will be double images.

4.2 Synthesis CNTs on AFM tip by floating Fe catalyst method

Fe particles and carbon source were mixed together in the solution form and were sprayed into the reactor. CNTs were grown from the Fe particles and then attached on the tip. Figure 4.1 shows a schematic view of synthesis of CNTs on AFM tip by floating Fe catalyst method. CVD condition is shown in table 4.1. CVD growth time was varied in 5, 10, 15 and 25 min, respectively [10].

This material is reserved for educational use only, not allowed for commercial use.
Forbidden to modify the content, and cite the document when use.

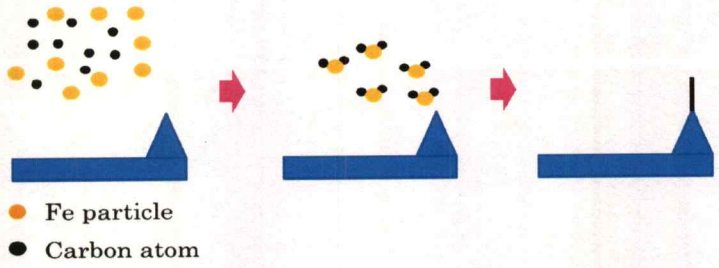

Figure 4.1 Schematic views of synthesis CNTs on AFM tip by floating Fe catalyst.

Table 4.1 CVD condition for growth of CNTs by floating Fe catalyst (CVD condition C1)

Carbon source and catalyst solution	: Ethanol 99 g, Ferrocene 1 g , Thiophene 0.157 g
Temperature	: 800°C
CVD Growth time	: 5, 10, 20, 25 min
Ar flow rate for ethanol bubbling	: 500 sccm
Ar flow rate for annealing	: 500 sccm

Synthesis of CNTs on AFM tip by floating Fe catalyst method provided too many CNTs on the tip. Thus, it is necessary to control density of CNTs. Selective catalyst deposition at the tip apex by using electroplating method is required.

4.3 Synthesis CNTs on AFM tip by electroplated Ni catalyst method

To attach CNT at the apex of cantilever by CVD method, prior to CVD process, it is necessary to deposit the metal catalyst film on the apex of pyramid shape of cantilever. In this study, Ni was selected as metal catalyst and electroplating was used for Ni deposition [16, 17]. Figure 4.2 shows schematic view of CNT growth on used-AFM cantilever.

This material is reserved for educational use only, not allowed for commercial use.
Forbidden to modify the content, and cite the document when use.

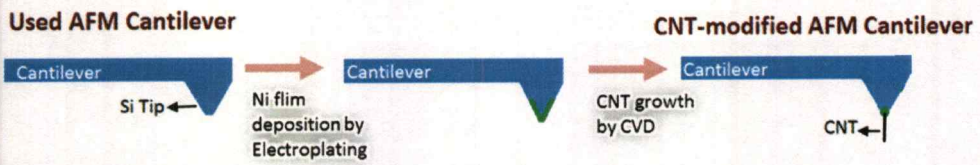

Figure 4.2 Schematic view of CNT growth on used-AFM cantilever.

4.3.1 Design of AFM Cantilever Fixture for Electroplating

Design of AFM cantilever fixture for Ni electroplating method is very important because it is desired to selectively deposit Ni film on tip apex (Si pyramid shape) only. Sharp materials have high density of electric field so Ni can attach on the tip apex area. AFM cantilever fixture was designed to fix cantilever and keep it floating on plating solution. Each AFM cantilever was set in the direction that its pyramid part pointing down to plating solution. A foam sheet was cut in rectangle shape and stainless steel (SS) sheets were fixed at both left and right sides of a foam sheet.

A foam sheet supports each cantilever to float in the same horizontal level during electroplating. When conduct electroplating, cantilever was fixed on the SS sheet by adhesive tape and conductive wire was connected between the SS sheet and the direct-current (DC) power supply. Figures 4.3 and 4.4 show schematic views of side and top views of the AFM cantilever fixture, respectively.

This material is reserved for educational use only, not allowed for commercial use.
Forbidden to modify the content, and cite the document when use.

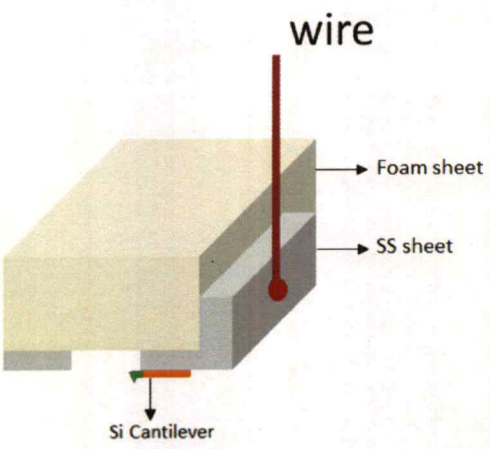

Figure 4.3 Schematic view of side view of the fixture showing that Si cantilever is set on the fixture.

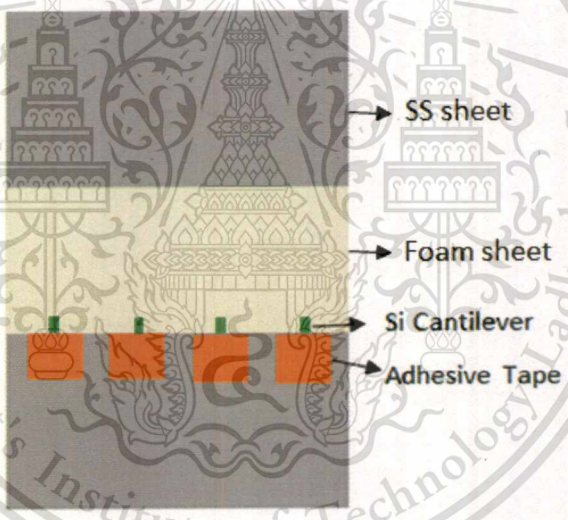

Figure 4.4 Schematic view of top view of the fixture.

This material is reserved for educational use only, not allowed for commercial use.
Forbidden to modify the content, and cite the document when use.

4.3.2 Synthesis CNTs on AFM tip by electroplated Ni catalyst.

In this study, electroplating method was adopted for Ni film deposition. This method is simple and does not need vacuum system such as sputtering or e-beam evaporation. Especially, this method can provide a selective deposition at the tip apex due to the high density of electric field at the tip apex according to its sharpness. Figure 4.5 shows setup of Ni electroplating. Ni film was deposited on the cantilever using DC electroplating technique. A commercial Ni electroplating bath was used as electrolyte in an electroplating process. Pyramid shape of cantilever was pointed down to plating solution. The used AFM cantilever was connected to the cathode while the Ni metal bar was connected to the anode of the circuit.

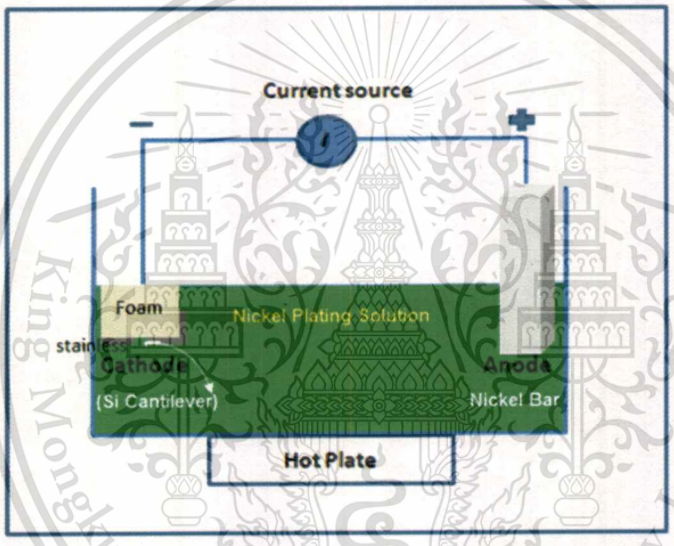

Figure 4.5 Setup of Ni electroplating for Ni film coating on Si cantilever.

4.3.2.1 Investigation of optimal condition for Ni electroplating

Effect of distance between anode and cathode and effect of plating time were investigated.

Si AFM cantilever was used as the cathode while Ni bar was used as the anode. Distance between anode and cathode were varied at 8 and 13 cm while the plating

This material is reserved for educational use only, not allowed for commercial use.
Forbidden to modify the content, and cite the document when use.

time were varied at 6, 12 and 30 s. Voltage, current, temperature parameters of electroplating were fixed at 1.4 V, 0.01 A and 40°C, respectively. The parameter values used in this experiment were referred from the reference papers [16, 17, 40]. After electroplating, cantilever was cleaned by dipping in deionized water approximately 15 s and drying by N_2 blow. Figure 4.6 shows schematic view of mechanism of Ni electroplating at AFM tip. Table 4.2 is Ni electroplating condition for electrode distance variation (Electroplating condition E1). Table 4.3 is Ni electroplating condition for electroplating time variation (Electroplating condition E2).

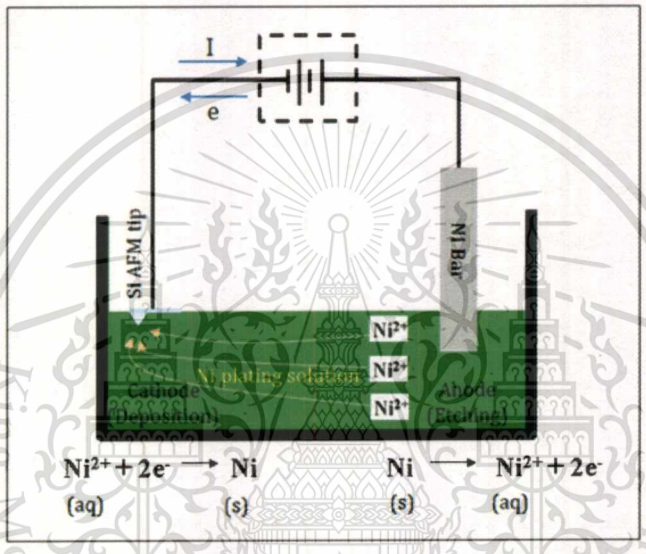

Figure 4.6 Mechanism of Ni electroplating at AFM tip.

Table 4.2 Ni electroplating condition for electrode distance variation (Electroplating condition E1)

Current	: 0.01 A
Voltage	: 1.40 V
Plating time	: 6 s
Distance between cathode and anode	: 8 , 13 cm
Ni solution temperature	: 40°C

This material is reserved for educational use only, not allowed for commercial use.
Forbidden to modify the content, and cite the document when use.

Table 4.3 Ni electroplating condition for electroplating time variation (Electroplating condition E2)

Current	: 0.01 A
Voltage	: 1.40
Plating time	: 6, 12, 30 s
Distance between cathode and anode	: 13 cm
Ni solution temperature	: 40°C

The shape and the contour of the object can affect the thickness of the plated layer. Cantilever with a pyramid shape which has a sharp tip will tend to have thicker plated deposits on the outside corners and thinner deposits in the recessed areas. This occurs because the DC current flows more densely around the outer edges of an object than the less accessible recessed areas.

4.3.2.2 Investigation of optimal condition for synthesis of CNTs on used AFM Cantilever by chemical vapor deposition method

Ni metal catalyst film-deposited AFM cantilever was set into a quartz tube reactor for CVD process. For standard CVD process, the quartz tube was filled with Ar gas for 30 min. Then, cantilevers were heated to the growth temperature and were annealed for 35 min. After temperature reached to the desired temperature, ethanol vapor (99.99%) was switched into the furnace by Ar bubbling for 20 min. After the temperature was dropped to room temperature, the cantilevers were taken out from the furnace [10].

Figure 4.7 and 4.8 shows schematic view of CVD system using ethanol as a carbon source and time-temperature profile during CVD process, respectively.

This material is reserved for educational use only, not allowed for commercial use.
Forbidden to modify the content, and cite the document when use.

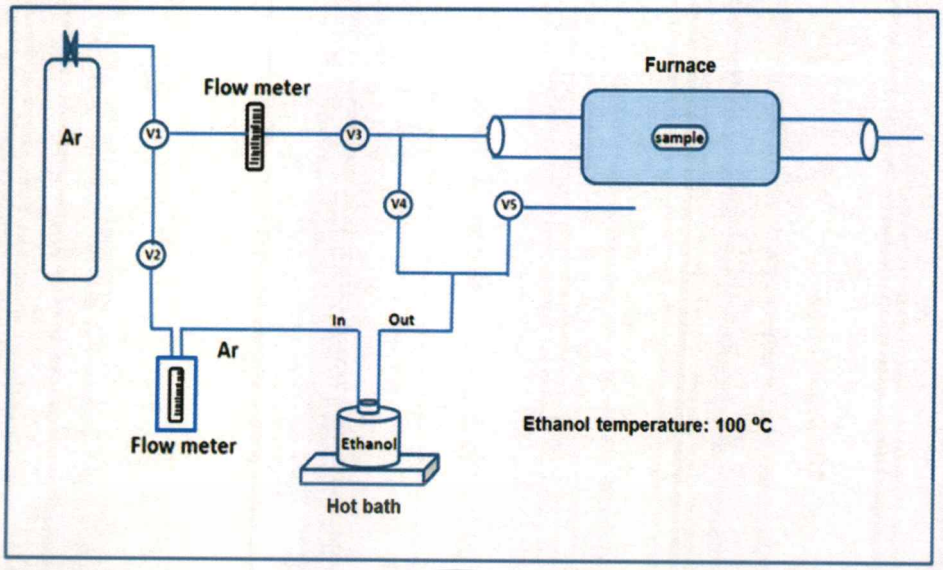

Figure 4.7 Schematic view of CVD system using ethanol as a carbon source.

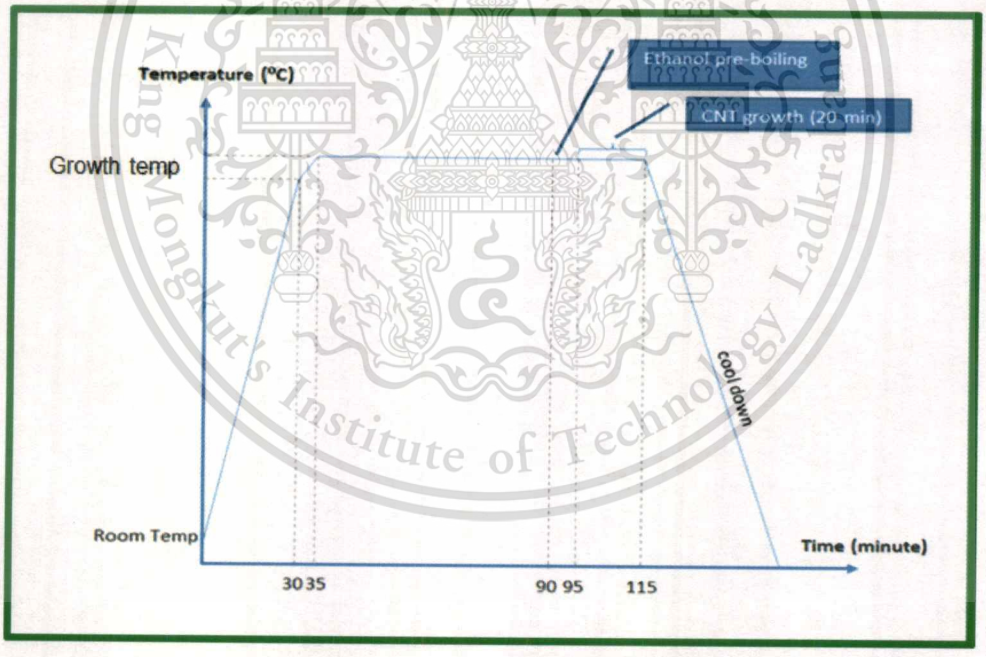

Figure 4.8 Time and temperature profile during CVD process.

This material is reserved for educational use only, not allowed for commercial use.
Forbidden to modify the content, and cite the document when use.

To investigate the effect of the electrode distance of Ni electroplating, the Ni-deposited AFM cantilevers was used as a platform for CNT grown under CVD condition shown in Table 4.4.

Table 4.4 CVD condition for investigation of effect of electrode distance (CVD condition C2)

Temperature	: 850°C
Growth time	: 10 min
Ethanol temperature	: 100°C
Ethanol flow rate	: 125 sccm
Ar flow rate	: 500 sccm
Sample position in the quartz tube	: center

To investigate the effect of the Ni electroplating time, the Ni-deposited AFM cantilevers was used as a platform for CNT grown under CVD condition shown in Table 4.5.

Table 4.5 CVD condition for investigation of effect of electroplating time (CVD condition C3)

Temperature	: 750°C
Growth time	: 10 min
Ethanol temperature	: 100°C
Ethanol flow rate	: 500 sccm
Ar flow rate	: 500 sccm
Sample position in the quartz tube	: center

To investigate the optimal condition for synthesis of CNTs on used AFM cantilever by CVD, effect of ethanol bubbling flow rate, CVD temperature and sample position were investigated and each condition was shown in Tables 4.6-4.8, respectively. The Ni electroplating condition was fixed by the condition shown in Table 4.9.

This material is reserved for educational use only, not allowed for commercial use.
Forbidden to modify the content, and cite the document when use.

Table 4.6 CVD condition for investigation of ethanol bubbling flow rate (CVD condition C4)

Temperature	: 750°C
Growth time	: 20 min
Ethanol temperature	: 100°C
Ethanol flow rate	: 125, 500 sccm
Ar flow rate	: 500 sccm
Sample position in the quartz tube	: center

Table 4.7 CVD condition for investigation effect of CVD temperature (CVD condition C5)

Temperature	: 750, 850°C
Growth time	: 20 min
Ethanol temperature	: 100°C
Ethanol flow rate	: 125 sccm
Ar flow rate	: 500 sccm
Sample position in the quartz tube	: center

Table 4.8 CVD condition for investigation of effect of position (CVD condition C6)

Temperature	: 850°C
Growth time	: 20 min
Ethanol temperature	: 100°C
Ethanol flow rate	: 125 sccm
Ar flow rate	: 500 sccm
Sample position in the quartz tube	: left, center, right

Table 4.9 Ni electroplating condition for investigation of the optimal CVD condition (Electroplating condition E3)

Current	: 0.01 A
Voltage	: 1.40
Plating time	: 6 s
Distance between cathode and anode	: 13 cm
Ni solution temperature	: 40°C

This material is reserved for educational use only, not allowed for commercial use.
Forbidden to modify the content, and cite the document when use.

Figure 4.9 shows a schematic view of sample position in the quartz tube for CVD system. The length of the heater area is 30 cm.

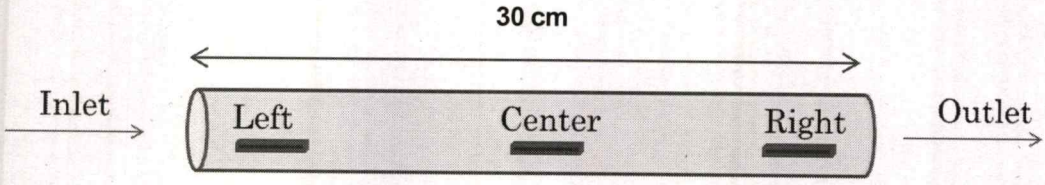

Figure 4.9 Schematic view of position in the quartz tube for CVD system.

Table 4.10 is a summary of combination of electroplating conditions and CVD conditions used in this research.

Table 4.10 A summary of electroplating and CVD conditions

Sample Set	Electroplating Condition	CVD Condition
1. Floating catalyst method		C1
2. Ni electroplating condition (parameter: electrode distance)	E1	C2
3. Ni electroplating condition (parameter: electroplating time)	E2	C3
4. CVD condition (parameter: ethanol bubbling flow rate)	E3	C4
5. CVD condition (parameter: CVD temperature)	E3	C5
6. CVD condition (parameter: sample position)	E3	C6

This material is reserved for educational use only, not allowed for commercial use.
Forbidden to modify the content, and cite the document when use.

4.4 Characterizations

4.4.1 Field Emission Scanning Electron Microscopy: FESEM

FESEM was used for characterization of morphology properties of catalyst nanoparticles, multi-walled carbon nanotubes (MWNTs), AFM cantilever and AFM standard sample. The model of FESEM that used in this research is FEI Sirion FESEM, NPGS v.9, EDAX Falcon. The FESEM specifications are shown in table 4.11.

Table 4.11 Specifications of FESEM

Pressure (analytical chamber)	6.3×10^{-6} mBar
Acceleration voltage (A.V.)	30 kV
Magnification	40 - 1,200,000X
Beam current	> 25 nA (A.V. 10 kV), > 0.5 pA (A.V. 500 eV)

4.4.2 High Resolution Transmission Electron Microscopy: HRTEM

HRTEM was used for characterization of MWNT structure. For sample preparation, CNTs on AFM cantilever apex were smeared from AFM tip to Cu grid. The model of HRTEM that used in this research is FEI TECNAI G2 20. The HRTEM specifications are shown in table 4.12.

Table 4.12 Specifications of HRTEM

Pressure (analytical chamber)	$< 2.7 \times 10^{-5}$ Pa
Acceleration voltage (A.V.)	200 kV
Magnification	25 – 700 kX
Filament type	LaB_6 emitter

This material is reserved for educational use only, not allowed for commercial use.
Forbidden to modify the content, and cite the document when use.

4.4.3 Raman spectrometer

Raman spectrometer was used for characterization of structure properties of MWNTs and carbon bonding. The model of Raman spectrometer that used in this research is DXR Smart Raman Spectrometer, Thermo Scientific. The Raman spectrometer specifications are shown in table 4.13.

Table 4.13 Specifications of Raman spectrometer

Excitation energy	532 nm (2.45 eV)
Excitation power	5 mW
Exposure time	2 s
Acquisition time	15 times

4.5 AFM Imaging performance test using CNT-modified AFM Cantilever

To evaluate the AFM imaging performance of the CNT-modified cantilever, the CNT-modified cantilever was used to scan the silicon dioxide coated with a uniform layer of platinum which is AFM standard sample (VLSI standard sample, STS2-180P). Atomic force microscopy (BRUKER, Dimension Icon) was utilized for AFM imaging in tapping mode. Cantilever data are thickness of 4 μm, length of 125 μm, width of 40 μm, resonance frequency (f_0) of 320 kHz and spring constant (k) of 42 N/m. For AFM imaging comparison, used and new cantilevers were also employed for imaging scanning. The scanned images and line profiles were used for comparison. After imaging scanning, the CNT-modified cantilever was observed by FESEM again to confirm its durability. Table 4.14 shows conventional AFM cantilever (Bruker, TESP) data.

This material is reserved for educational use only, not allowed for commercial use.
Forbidden to modify the content, and cite the document when use.

Table 4.14 Conventional AFM cantilever (Bruker, TESP) data

Technical data	Value	Range
Thickness (μm)	4 μm	3.5 – 4.5
Mean width (μm)	40 μm	25.0 – 45.0
Length (μm)	125 μm	110.0 – 140.0
Force constant (N/m)	42 N/m	20.0 – 80.0
Resonance Frequency (kHz)	320 kHz	200.0 – 410.0
Curvature radius (nm)	58 nm	
Mode of operation	Tapping	

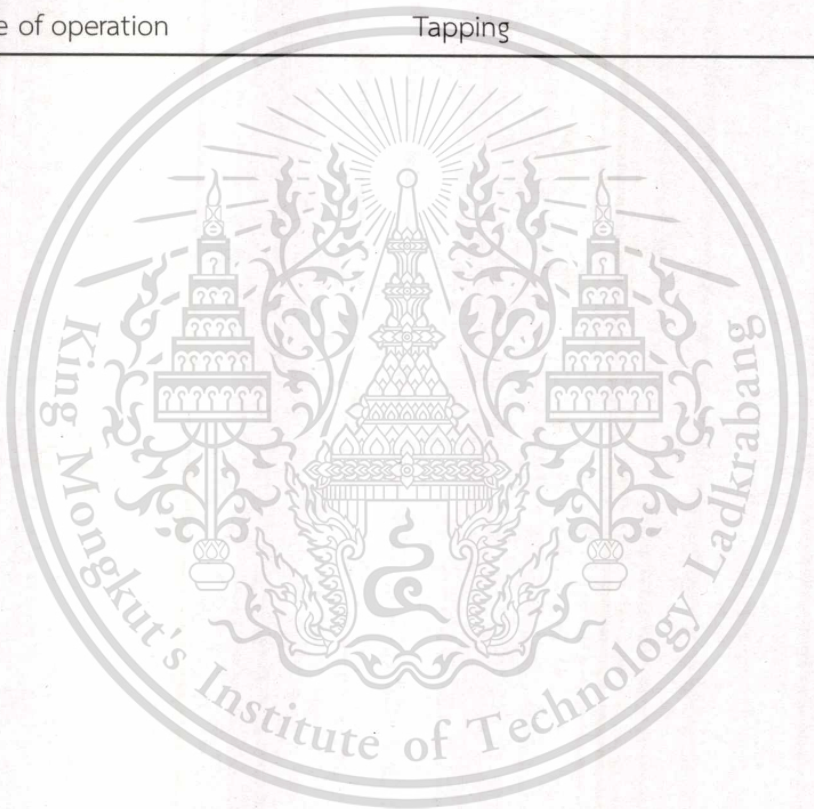

This material is reserved for educational use only, not allowed for commercial use.
Forbidden to modify the content, and cite the document when use.

Chapter 5

RESULTS AND DISCUSSION

This chapter describes the results of fabrication of CNT-modified used AFM cantilever. Field emission scanning electron microscopy (FESEM), high resolution transmission electron microscopy (HRTEM), Raman spectrometer were utilized to characterize morphology and structure of the synthesized CNTs on the apex of pyramid shape of AFM cantilever. AFM imaging performance of the CNT-modified used AFM cantilever was investigate using AFM standard sample as a sample test. The obtained image and line profile was compared with those obtained by used and new cantilevers.

5.1 Characterization of used AFM cantilever for experiment

Figure 5.1 shows examples of FESEM images of used AFM tips before electroplating and chemical vapor deposition. Used AFM cantilevers that are appropriate for the experiment, should have curvature radius approximately 60 - 150 nm (Figures 5.1 (a)-(c)). Used AFM tips those were broken or contaminated, were not used in the experiment (figures 5.1 (d)-(i)). When broken tips were used for image scanning, the AFM imaging was not clear and showed double images as shown in figure 5.2.

This material is reserved for educational use only, not allowed for commercial use.
Forbidden to modify the content, and cite the document when use.

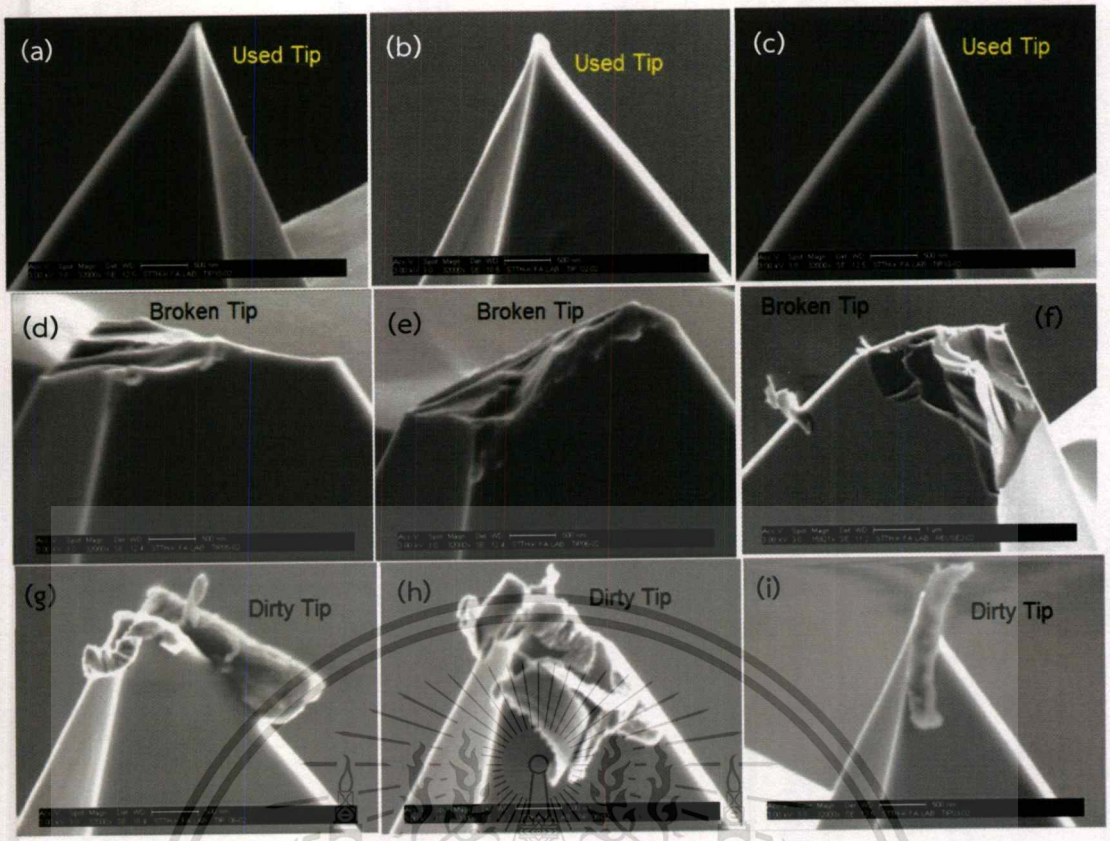

Figure 5.1 Examples of FESEM images of used AFM tips
(a)-(c) used tip for CNTs growth, (d)-(f) broken tips and (g)-(i) contaminated tips

Figure 5.2 AFM image obtained from broken used AFM tip.
(a) 2D image and (b) 3D image

This material is reserved for educational use only, not allowed for commercial use.
Forbidden to modify the content, and cite the document when use.

5.2 FESEM Characterization of CNTs on AFM tip by floating Fe catalyst method

Figure 5.3 shows FESEM images of used cantilevers after CVD process by Fe floating catalyst CVD at different growth times. CVD condition is shown in table 4.1. CVD growth time was varied in 5, 10, 20 and 25 min, respectively.

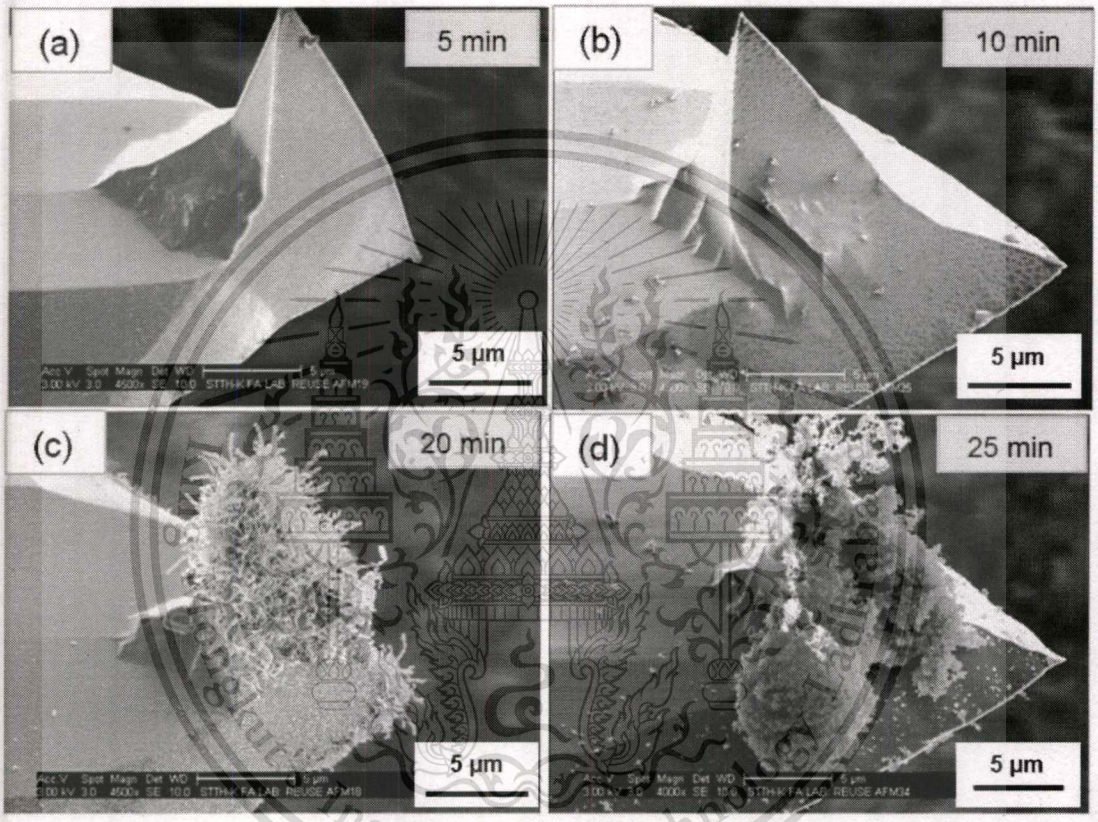

Figure 5.3 FESEM images of synthesized CNTs on used AFM cantilever by Fe floating catalyst CVD at different growth times; (a) 5, (b) 10, (c) 20 and (d) 25 min

Growth times of 5 and 10 min gave low density of CNTs at cantilever body and no CNT on the apex of the tip. Growth times of 20 and 25 min gave high density of CNTs covered tip apex. Figure 5.4 shows FESEM images at high magnification of CNT-modified AFM cantilever by floating Fe catalyst method.

This material is reserved for educational use only, not allowed for commercial use.
Forbidden to modify the content, and cite the document when use.

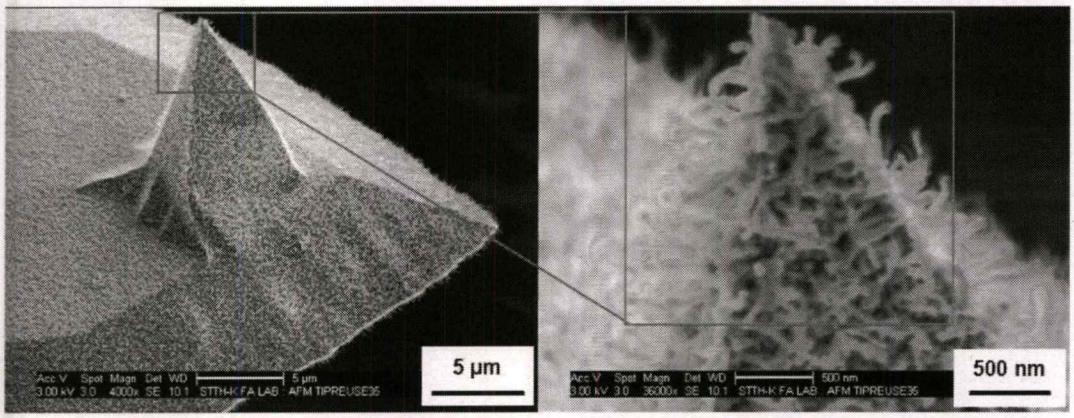

Figure 5.4 FESEM images at high magnification of CNT-modified AFM cantilever by floating Fe catalyst method.

From figure 5.4, FESEM images at high magnification of CNT-modified AFM cantilever by floating Fe catalyst method, shows too many CNTs on the tip, so it is necessary to control density of CNTs. Selective catalyst deposition at the tip apex by using electroplating method is a promising method.

5.3 Characterization of CNTs on AFM tip by electroplated Ni catalyst

5.3.1. Optimal condition for Ni electroplating

5.3.1.1 Effect of electrode distance

Effect of distance between anode and cathode was investigated; 8 and 13 cm. The electroplating and CVD conditions are shown in tables 4.2 and 4.4, respectively. Figure 5.5 show FESEM images of the CNTs synthesized from electroplated Ni catalyst deposited at different electrode distances.

This material is reserved for educational use only, not allowed for commercial use.
Forbidden to modify the content, and cite the document when use.

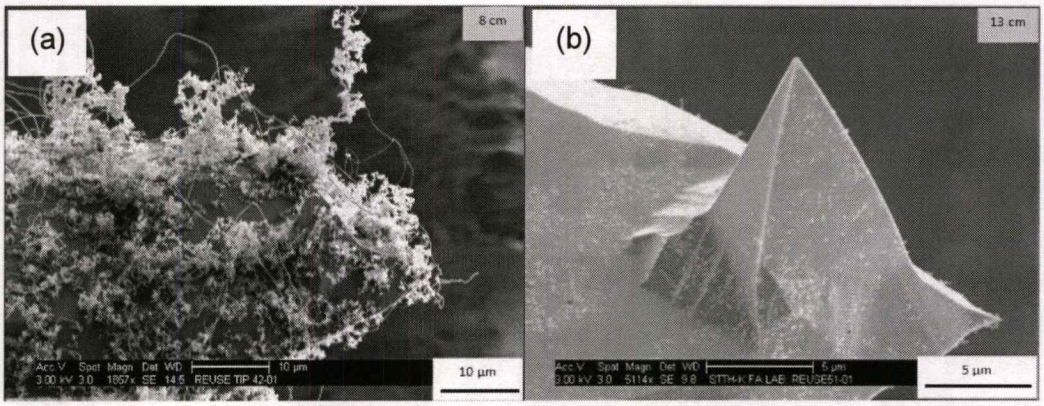

Figure 5.5 FESEM images of the CNTs synthesized from electroplated Ni catalyst deposited at different electrode distances; (a) 8 and (b) 13 cm

From figure 5.5, electrode distance of 8 cm shows high density of CNTs covered cantilever while electrode distance of 13 cm shows low density of CNTs only on cantilever body.

5.3.1.2 Effect of electroplating time

Effect of plating time was investigated; 6, 12 and 30 s. The electroplating and CVD conditions are shown in tables 4.3 and 4.5, respectively. Figure 5.6 show FESEM images of the CNTs synthesized from electroplated Ni catalyst deposited at different electroplating times.

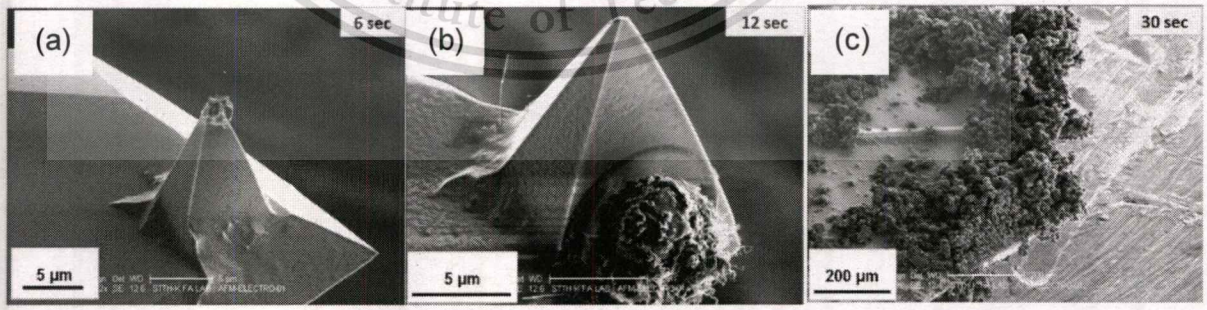

Figure 5.6 FESEM images of the CNTs synthesized from electroplated Ni catalyst deposited at different electroplating times; (a) 6, (b) 12 and (c) 30 s.

This material is reserved for educational use only, not allowed for commercial use.
Forbidden to modify the content, and cite the document when use.

From figure 5.6, electroplating time of 6 and 12 s shows low density at the tip while electroplating time of 30 s shows high density of CNTs covered cantilever.

Thus, electrode distance of 13 cm and electroplating time of 6 s is an optimal condition for synthesis of CNTs on used AFM cantilever.

5.3.2. Optimal condition for CVD

5.3.2.1 Effect of ethanol bubbling flow rate

Effect of ethanol bubbling flow rate was investigated; 125 and 500 sccm. The electroplating and CVD conditions are shown in tables 4.9 and 4.6, respectively. Figure 5.7 show FESEM images of the CNTs synthesized from different ethanol bubbling flow rates.

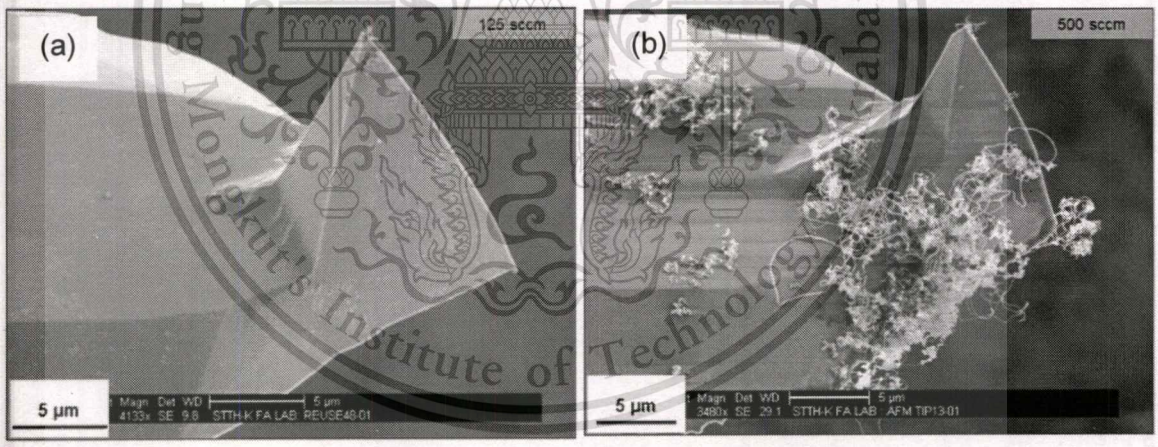

Figure 5.7 FESEM images of the CNTs synthesized from different ethanol bubbling flow rates; (a) 125 and (b) 500 sccm.

From figure 5.7, ethanol flow rate of 125 sccm shows a low density of CNTs at the tip while that of 500 sccm shows a low density of CNTs at the tip with a high density of CNTs at the cantilever body.

This material is reserved for educational use only, not allowed for commercial use.
Forbidden to modify the content, and cite the document when use.

5.3.2.2 Effect of CVD temperature

Effect of CVD temperature was investigated; 750 and 850°C. The electroplating and CVD conditions are shown in tables 4.9 and 4.7, respectively. Figure 5.8 show FESEM images of the CNTs synthesized from different CVD temperatures.

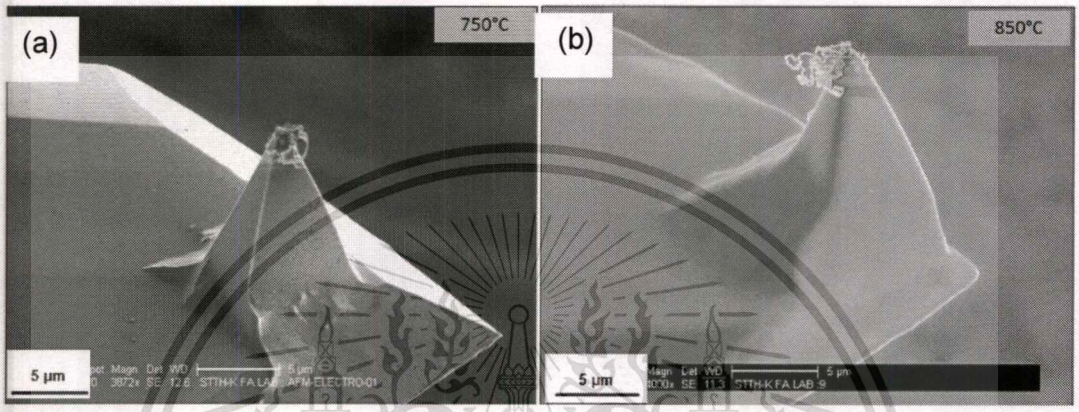

Figure 5.8 FESEM images of the CNTs synthesized from different CVD temperatures; (a) 750 and (b) 850°C.

From figure 5.8, CVD temperatures of 750 and 850°C show a low density of CNTs on the tip. There are no significant differences of CNT density at different CVD temperatures.

5.3.2.3 Effect of sample position

Effect of sample position was investigated; left, center and right position. The electroplating and CVD conditions are shown in tables 4.9 and 4.8, respectively. Figure 5.9 show FESEM images of the CNTs synthesized from different sample positions.

This material is reserved for educational use only, not allowed for commercial use.
Forbidden to modify the content, and cite the document when use.

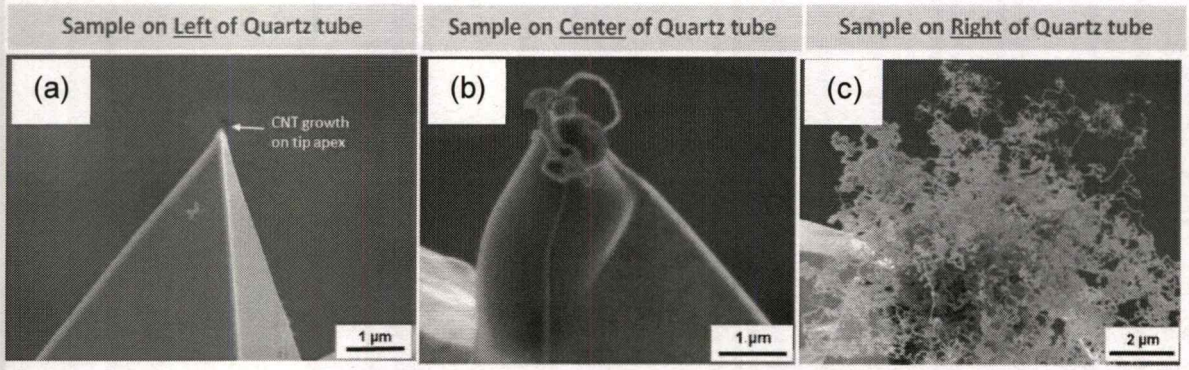

Figure 5.9 FESEM images of the CNTs synthesized from different sample positions; (a) left, (b) center and (c) right of quartz tube.

From Figure 5.9, left position shows one or two CNTs, center position shows a low density of CNTs and right position shows the highest density of CNTs.

From this study, the optimal condition for Ni electroplating of used AFM cantilever is shown in table 5.1 and the optimal condition for growth of CNT on AFM cantilever apex using CVD method is shown in table 5.2, respectively.

Table 5.1 The optimal condition for Ni electroplating on used AFM cantilever

Current	: 0.01 A
Voltage	: 1.40 V
Plating time	: 6 s
Distance between cathode and anode	: 13 cm
Ni solution temperature	: 40°C

Table 5.2 The optimal condition for growth of CNT on AFM cantilever apex using CVD method.

Temperature	: 850°C
Growth time	: 20 min
Ethanol temperature	: 100°C
Ethanol flow rate	: 125 sccm
Ar flow rate	: 500 sccm
Sample position in the quartz tube	: Left

This material is reserved for educational use only, not allowed for commercial use.
Forbidden to modify the content, and cite the document when use.

Figures 5.10 (a) - (c) show FESEM images of CNT-modified cantilevers at different magnifications of FESEM from the optimal electroplating and CVD conditions. CNTs were found at the tip apex of Si pyramid shape, the edge of Si pyramid shape and the edge of cantilever. Figure 5.11 shows FESEM images of other CNT-modified cantilevers grown from the optimal electroplating and CVD conditions.

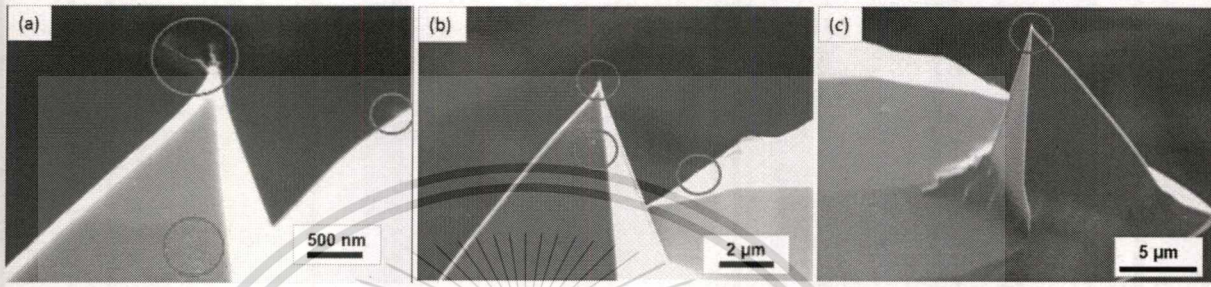

Figure 5.10 FESEM images of CNT-modified cantilevers at different magnifications of FESEM.

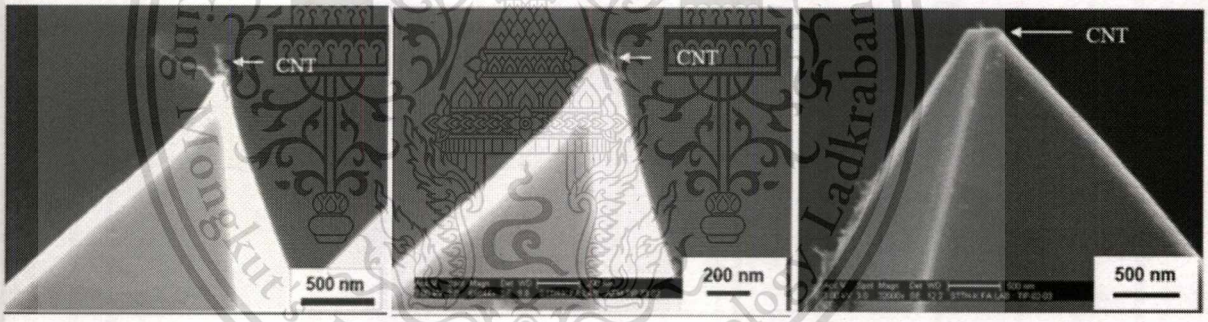

Figure 5.11 FESEM images of other CNT-modified cantilevers grown from the optimal electroplating and CVD conditions.

Figures 5.12 (a) - (c) show FESEM images of used, new and CNT-modified cantilevers, respectively.

This material is reserved for educational use only, not allowed for commercial use.
Forbidden to modify the content, and cite the document when use.

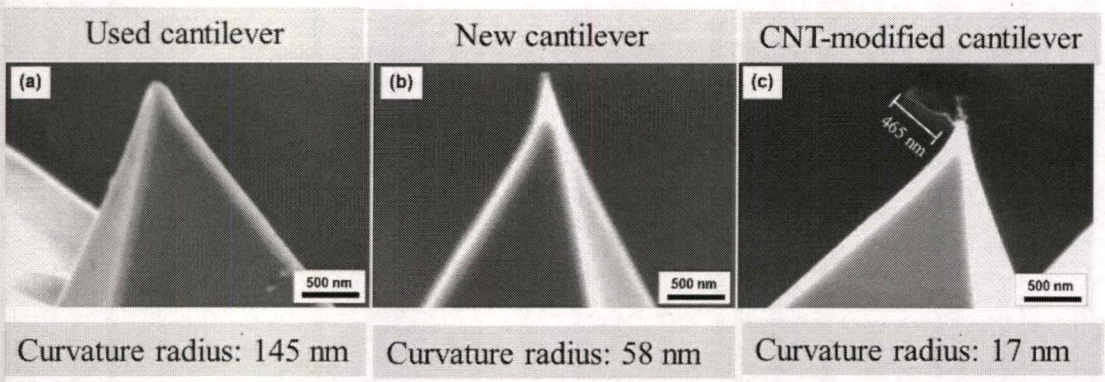

Figure 5.12 FESEM images of (a) used, (b) new and (c) CNT-modified cantilevers.

The curvature radius of each cantilever apex was different. Used cantilever had the dull apex with a curvature radius of 145 nm, while new cantilever had the relatively sharp apex with a curvature radius of 58 nm. For CNT-modified cantilever, CNTs with a thin tubular structure were protruded from apex of cantilever with a length of approximately 465 nm. The curvature radius of the used cantilever before CNT modification was approximately 87 nm. After modified used AFM cantilever, curvature radius was approximately 17 nm.

5.3.3 HRTEM Characterization of CNTs on AFM tip by electroplated Ni catalyst

For HRTEM observation, it is difficult to directly observe the structure of CNT protruded from cantilever apex. To obtain the trend of the resultant CNTs, CNTs on cantilever were smeared to Cu grid and characterized. Thus, not only the CNTs at the apex, but also CNTs at the cantilever body were observed. Figures 5.13 show HRTEM images of CNT on used cantilever after CVD process.

This material is reserved for educational use only, not allowed for commercial use.
Forbidden to modify the content, and cite the document when use.

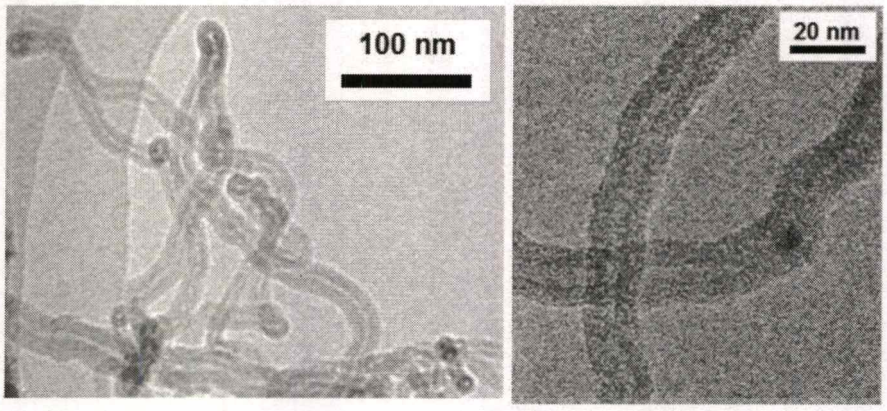

Figure 5.13 HRTEM images of CNT-modified cantilever.

It was found that the resultant CNTs consisted of graphite layers, implying multi-walled carbon nanotube (MWCNT) structure [41]. The high contrast in the image was assumed to be Ni catalyst. Diameters of MWNTs were approximately estimated to be with a diameter of 17.29±0.59 nm. From, HRTEM it cannot determine the growth mode of the CNTs.

5.3.4 Raman Spectrometer Characterization of CNTs on AFM tip by electroplated Ni catalyst

The CNT-modified cantilever was characterized by Raman spectrometer by using an Ar ion laser with a wavelength of 532 nm (2.45 eV) and a power of 5 mW. The laser was focused at the apex of modified CNT AFM tip. Figure 5.14 shows Raman spectrum obtained from CNT-modified AFM tip at high-frequency region.

There are two important peaks of CNTs. *D* peak is approximately 1350 cm^{-1} and *G* peak is approximately 1590 cm^{-1}, which can be reasonably assigned to disorder-induced (*D*) mode and C-C stretching (*G*) mode of graphite structure, respectively.

This spectrum implies the MWCNT structure. The intensity ratio of *G*-band to *D*-band is usually used for evaluating the quality of the produced CNTs. The higher ratio of intensity of *G*-band to *D*-band indicates the higher crystallinity and purity of the produced CNTs [10, 17]. The intensity ratio of *G*-band to *D*-band of this MWCNT is approximately 1.38.

This material is reserved for educational use only, not allowed for commercial use.
Forbidden to modify the content, and cite the document when use.

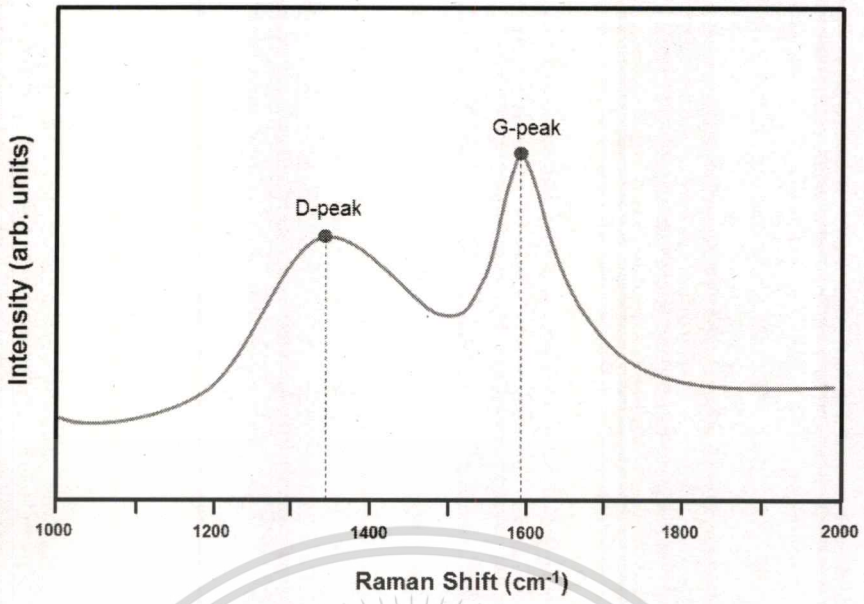

Figure 5.14 Raman spectrum obtained from CNT-modified AFM tip.

5.4 AFM Imaging using CNT-modified AFM Cantilever

5.4.1 AFM standard sample

For AFM imaging performance test, the CNT-modified cantilever was used to scan silicon dioxide coated with a uniform layer of platinum which is AFM standard sample (VLSI standard sample, STS2-180P). Images were scanned in tapping mode. Cantilever had thickness of 4 μm, length of 125 μm, width of 40 μm, resonance frequency (f_0) of 320 kHz and spring constant (k) of 42 N/m. For AFM imaging comparison, used and new cantilevers were also employed for imaging scanning. Figure 5.15 shows FESEM image of AFM standard sample. Figure 5.16 shows schematic view of line profile measurement of height, pitch and angle of standard sample. Table 5.3 shows specifications of the standard sample.

This material is reserved for educational use only, not allowed for commercial use.
Forbidden to modify the content, and cite the document when use.

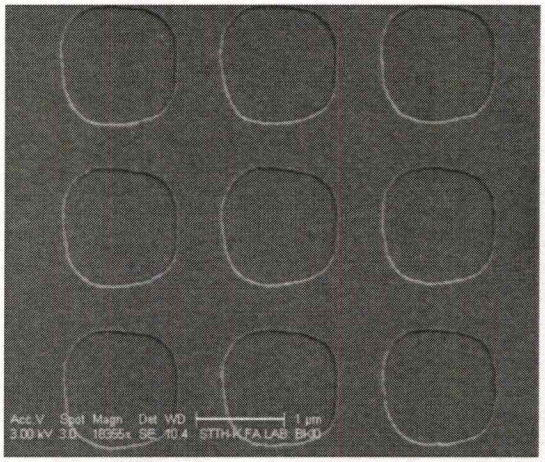

Figure 5.15 FESEM image of AFM standard sample.

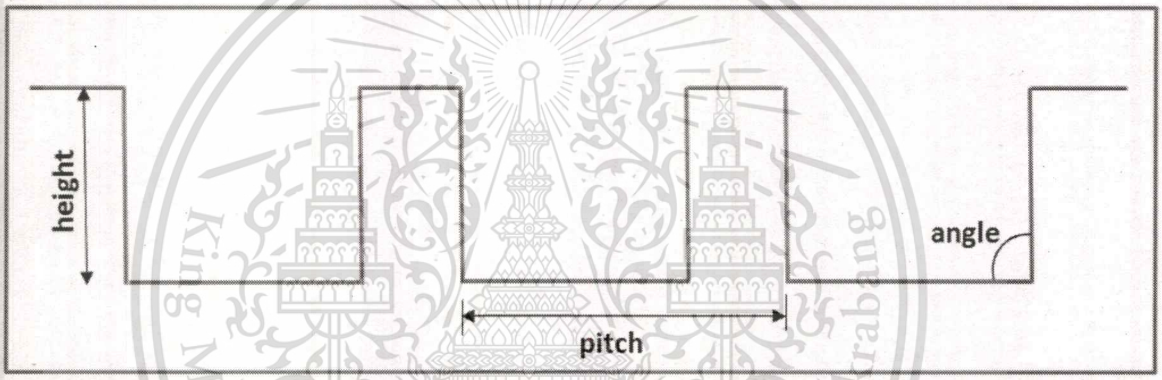

Figure 5.16 Schematic view of line profile measurement of height, pitch and angle.

Table 5.3 Specifications of the standard sample.

	Mean Height, Z (nm)	Mean Pitch, X (µm)	Mean Pitch, Y (µm)	Angle (degree)
Standard sample	18.400± 3.300	1.799± 0.023	1.799± 0.023	90.000°

This material is reserved for educational use only, not allowed for commercial use.
Forbidden to modify the content, and cite the document when use.

5.4.2 AFM Imaging Comparisons

For imaging scanning, each cantilever was scanned under the same AFM operation setting at a scan rate of 1 Hz, a set point of 250 mV, a scan size of 6 μm x 6 μm, samples/line of 512 and a scan angle of 90°. AFM scanning was conducted for 2 times for each cantilever. Figures 5.17 (a) - (f) show 2D and 3D AFM images of standard sample obtained by used, new and CNT-modified cantilever, respectively.

From figures 5.17 (a), (c) and (e), it can be obviously seen that the imagings from new and CNT-modified cantilever were clear, while the imaging from used cantilever was vague.

Figures 5.18 (a) - (c) show line profile of AFM image obtained from used, new and CNT-modified cantilevers, respectively. Average mean height, mean pitch and angle of each image were measured from its line profile of 9 pitches and were summarized in table 5.4. Differences of line profile of AFM images scanned by different cantilevers compared to standard sample specification were summarized in table 5.5. Table 5.6 shows percentage difference of average of mean height, mean pitch and angle of AFM image scanned by different cantilevers compared to standard sample specification. Figure 5.19 shows a pareto chart of percentage difference from the standard specification. Percentage differences of mean height scanned by CNT-modified, new and used AFM cantilevers are approximately are 0.91, 17.67 and 20.48%, respectively. Percentage differences of pitch X scanned by CNT-modified, new and used AFM cantilevers are approximately 0.22, 0.28 and 1.00%, respectively. Percentage differences of pitch Y scanned by CNT-modified, new and used AFM cantilevers are approximately are 1.28, 1.72 and 1.72%, respectively. Percentage differences of angle scanned by CNT-modified, new and used AFM cantilevers are approximately 2, 4 and 8%, respectively. These results show that CNT-modified cantilever provided scanned image with only 1 - 2% difference from the standard specification while used cantilever showed 2 - 20%.

Line profiles of the image obtained from CNT-modified cantilever show relatively same specification as that of standard sample, while that of used and new cantilevers showed the much difference especially in mean height, implying that

This material is reserved for educational use only, not allowed for commercial use.
Forbidden to modify the content, and cite the document when use.

superior to new and used AFM cantilevers, the CNT-modified AFM cantilevers exhibit high-resolution imaging in both lateral and vertical resolution.

Moreover, focusing at the line profile of the AFM image scanned by CNT-modified cantilever, it was found that surface of cavity showed roughness while the line profile of the AFM image scanned by new and used cantilever showed flat surface of cavity. These results also indicate that CNT-modified cantilever have higher resolution than new and used AFM cantilever in term of bottom roughness.

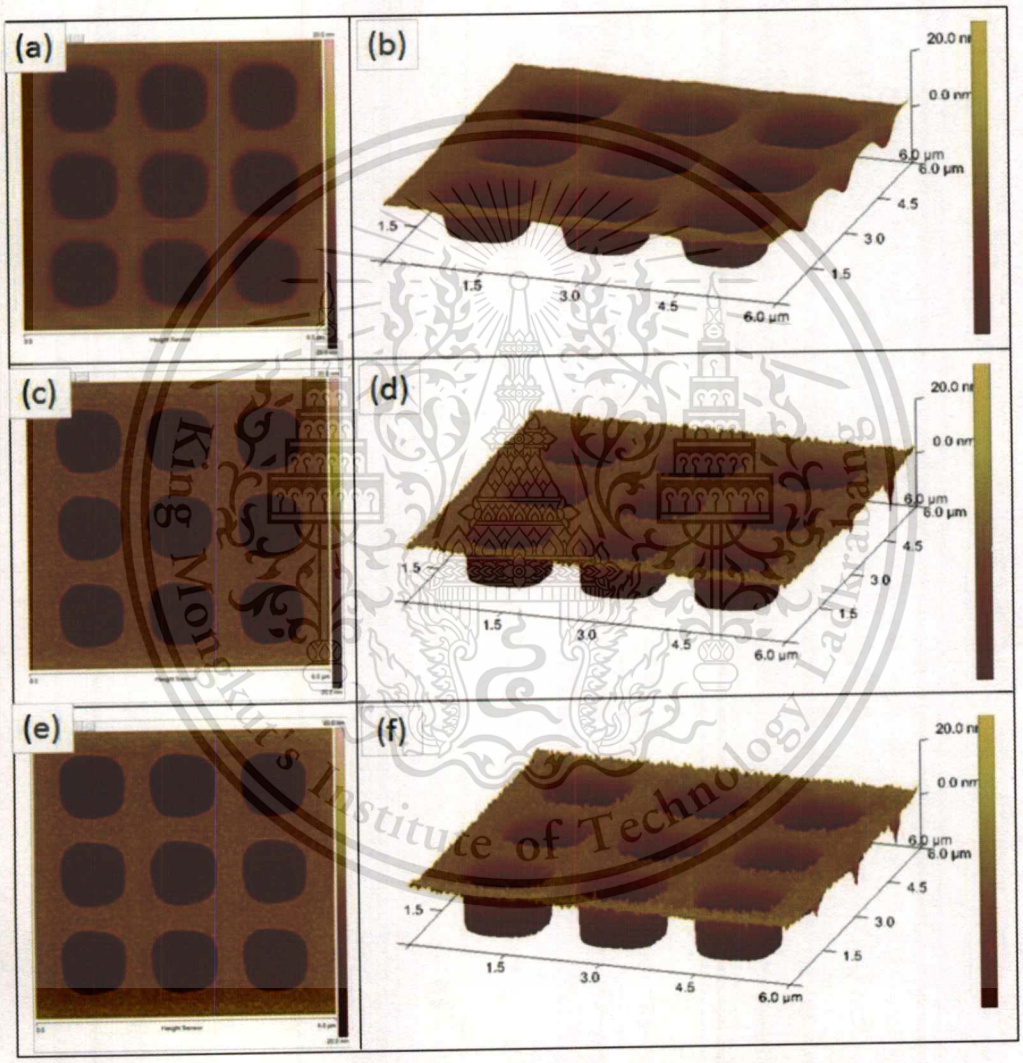

Figure 5.17 (a), (c), (e) 2D and (b), (d), (f) 3D AFM images of standard sample obtained by used, new and CNT-modified cantilevers, respectively.

This material is reserved for educational use only, not allowed for commercial use.
Forbidden to modify the content, and cite the document when use.

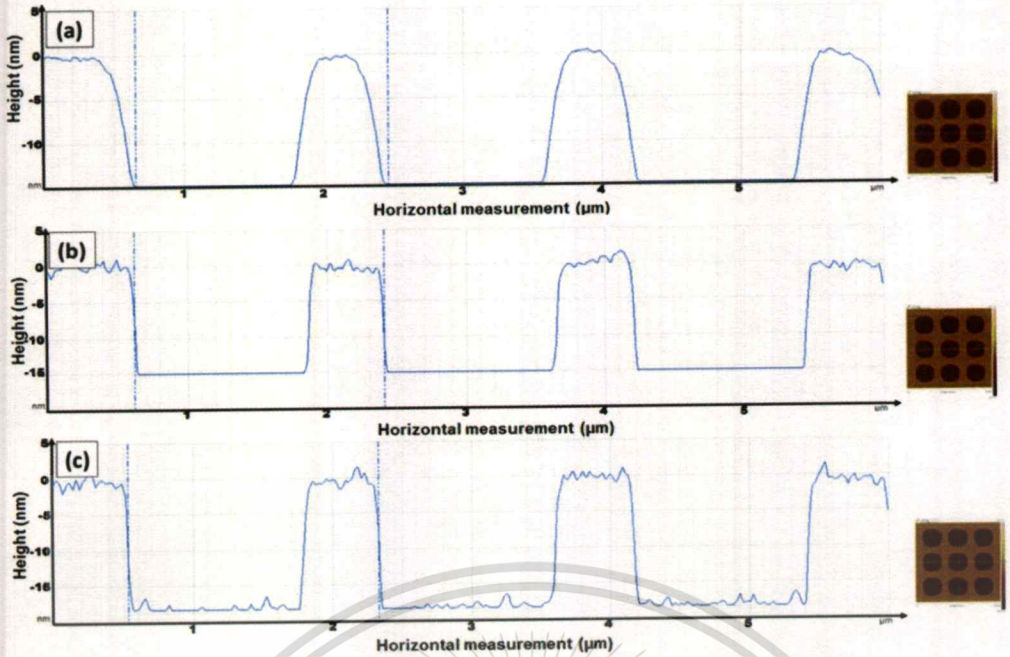

Figure 5.18 AFM line profiles using (a) used, (b) new and (c) CNT-modified cantilevers.

Table 5.4 Average mean height, mean pitch and angle of AFM image scanned by different cantilevers.

	Mean Height, Z (nm)	Mean Pitch, X (µm)	Mean Pitch, Y (µm)	Angle (degree)
Standard sample	18.400± 3.300	1.799± 0.023	1.799± 0.023	90.000°
Used cantilever	14.632± 0.185	1.817± 0.023	1.830± 0.016	97.610° ± 1.370
New AFM cantilever	15.148± 0.269	1.804± 0.017	1.830± 0.014	93.620° ± 2.230
CNT-Modified cantilever	18.568± 0.315	1.803± 0.013	1.822± 0.015	92.020° ± 1.630

This material is reserved for educational use only, not allowed for commercial use.
Forbidden to modify the content, and cite the document when use.

Table 5.5 Difference of average mean height, mean pitch and angle of AFM image scanned by different cantilevers compared to standard sample specification.

	ΔMean Height, Z (nm)	ΔMean Pitch, X (μm)	ΔMean Pitch, Y (μm)	ΔAngle (degree)
Used cantilever	3.768	0.018	0.031	7.610
New AFM cantilever	3.252	0.005	0.031	3.620
CNT-Modified cantilever	0.168	0.004	0.023	2.020

Table 5.6 Percentage difference of average mean height, mean pitch and angle of AFM image scanned by different cantilevers compared to standard sample specification.

	%delta of height	%delta of pitch X	%delta of pitch Y	%delta of angle
Used cantilever	20.48	1.00	1.72	8.46
New AFM cantilever	17.67	0.28	1.72	4.02
CNT-Modified cantilever	0.91	0.22	1.28	2.24

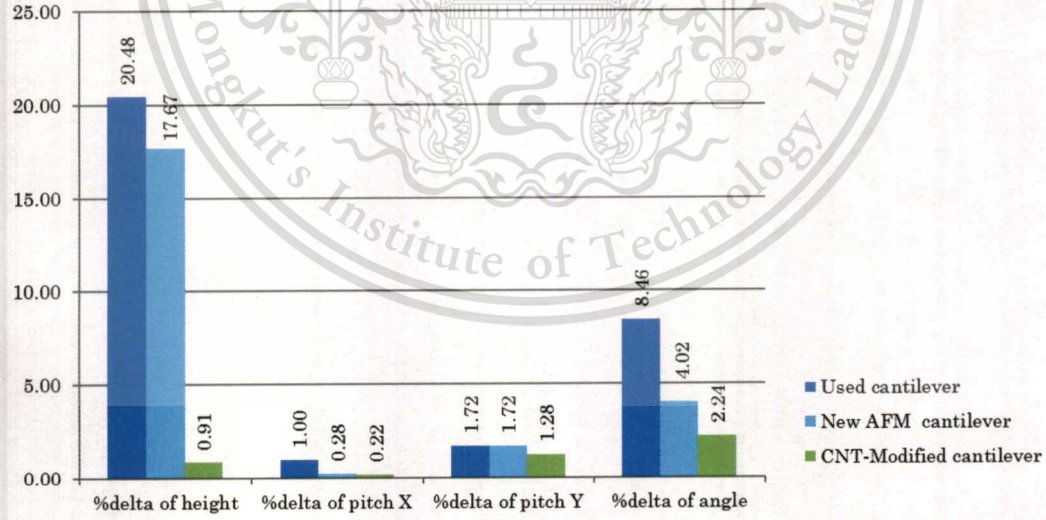

Figure 5.19 Pareto chart of percentage difference from the standard specification.

This material is reserved for educational use only, not allowed for commercial use.
Forbidden to modify the content, and cite the document when use.

5.4.3 Durability of CNT-modified AFM cantilever

To confirm the durability of CNT-modified cantilever, CNT-modified cantilever before and after AFM measurements were characterized by FESEM. Figures 5.20(a) and (b) show FESEM images of CNT-modified cantilever before and after AFM measurements.

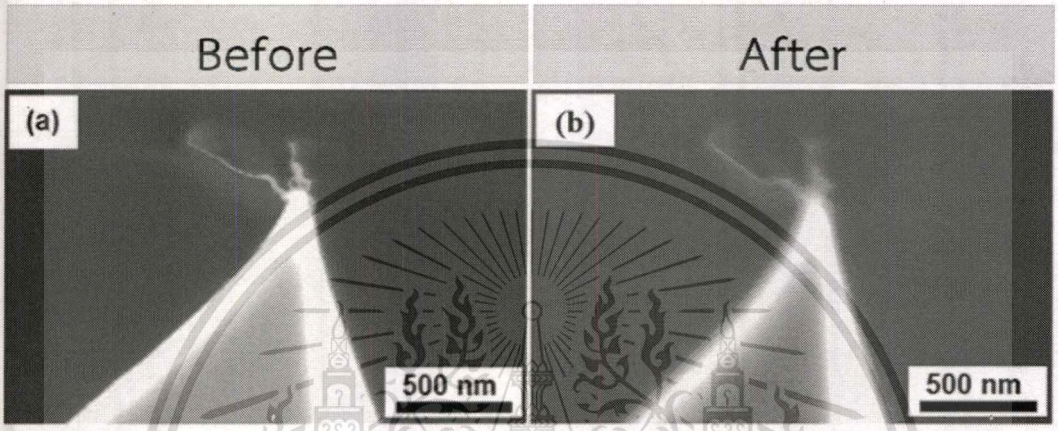

Figure 5.20 FESEM images of CNT-modified cantilever (a) before and (b) after AFM measurements.

FESEM image of CNT-modified cantilever before AFM imaging test showed two thin tubular structures were protruded from apex of cantilever. After AFM imaging test for two times, CNT-modified cantilever was characterized by FESEM again. The results show that CNTs still stick on the cantilever, implying that CNT-modified cantilever has durability and long life time due to excellent mechanical properties of CNT.

This material is reserved for educational use only, not allowed for commercial use.
Forbidden to modify the content, and cite the document when use.

5.5 Yield of synthesis of CNT-modified AFM cantilever

In this research, 11 cantilevers were used for CNT synthesis under the optimal electroplating and CVD conditions (table 5.1 and 5.2). Figure 5.21 shows FESEM images of used cantilevers after CVD under the optimal conditions.

After CVD, there are 7 cantilevers that have CNTs on the tip apex of AFM cantilevers as shown in figures 5.21 (a)-(g). Thus, yield of synthesis of CNTs on used AFM cantilever [42] is approximately 64%.

However, for AFM imaging, there should be only 1-2 CNTs on the tip apex. After CVD, there are 3 cantilevers that are suitable for AFM cantilever application as shown in figures 5.21 (a)–(c). Yield of synthesis of CNT-modified AFM cantilever [42] is approximately 27%.

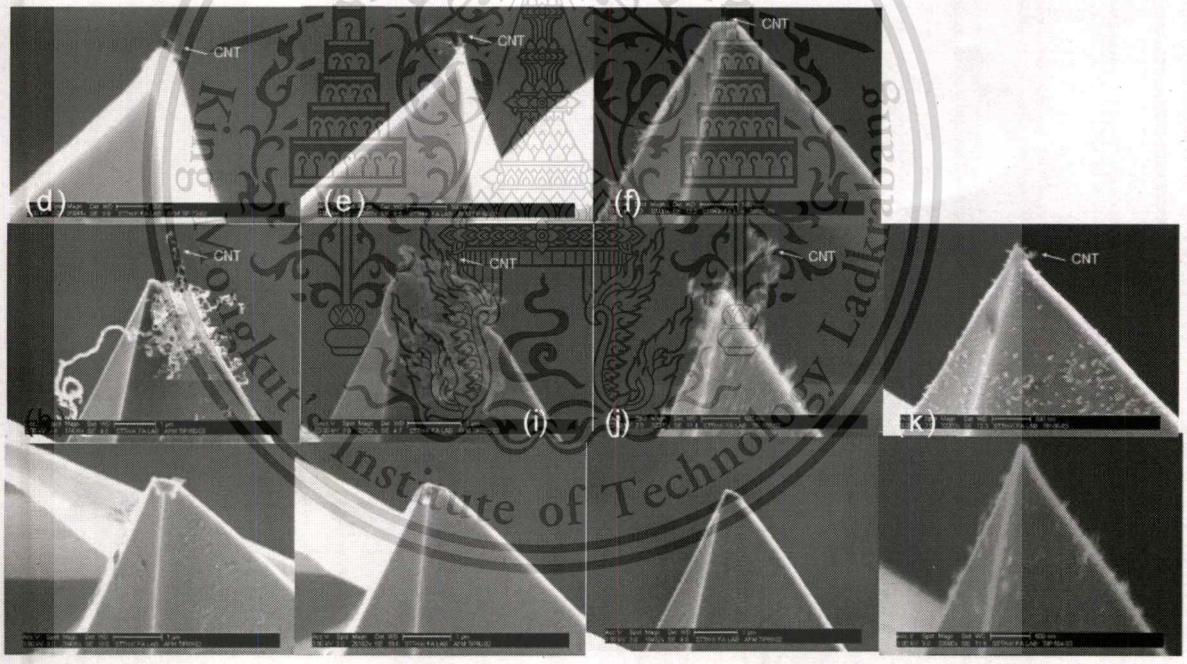

Figure 5.21 FESEM images of used cantilevers after CVD under the optimal conditions.

A low yield of synthesis of CNT-modified AFM cantilever may be attributed to the reproducibility of the optimal condition of Ni electroplating. The Ni electroplating time is 6 s, thus it is difficult to precisely control due to our device limitation.

This material is reserved for educational use only, not allowed for commercial use.
Forbidden to modify the content, and cite the document when use.

Chapter 6

CONCLUSION

AND SUGGESTIONS FOR FUTURE RESEARCH

Modification of used atomic force microscope (AFM) cantilever by carbon nanotube (CNT) attachment and its imaging performance was demonstrated. Used Si AFM cantilever is a dull tip or an apex-damaged tip. AFM imaging obtained from these used cantilevers is not clear and low resolution. Used AFM cantilevers that are appropriate for the experiment, should have curvature radius approximately 60 - 150 nm.

In this study, the used cantilever was modified by attaching CNT on the Si pyramid shape of cantilever by direct growth, using floating Fe catalyst and Ni catalyst-assisted chemical vapor deposition (CVD) method.

First, attachment of CNTs on the tip of the used cantilever using floating Fe catalyst was investigated. The synthesized CNTs at the tip were high density. A high density of CNTs on the tip is not appropriate for AFM imaging. Thus, it is necessary to control density of CNTs. Selective catalyst deposition at the tip apex by using electroplating method is required.

Second, attachment of CNTs on the tip of the used cantilever using Ni catalyst was investigated. Design of AFM cantilever fixture is very important because it is desired to selectively deposit Ni film on tip apex (pyramid shape). AFM cantilever fixture was designed to fix cantilever and keep it floating on plating solution during Ni electroplating process. Each AFM cantilever was set in the direction that its pyramid part pointing down to plating solution. The optimal condition for Ni electroplating was investigated. Effect of distance between anode and cathode, and plating time were studied. The optimal electroplating was performed at Ni plating solution temperature of 40°C for 6 s at the applied voltage of 1.4 V, current of 0.01 A and the distance between anode and cathode of 13 cm. For CVD process, ethanol was used as carbon source. The optimal condition for CVD process was investigated. Effect of

This material is reserved for educational use only, not allowed for commercial use.
Forbidden to modify the content, and cite the document when use.

ethanol bubbling flow rate, CVD temperature and sample position were studied. The optimal CVD was performed at growth temperature of 850°C for 20 min at the position of the left side of quartz tube under the ethanol bubbling flow rate of 125 sccm. Field emission scanning electron microscope (FESEM), high resolution transmission electron microscope (HRTEM) and Raman spectrometer were utilized for the synthesized CNT characterization. There were 1-2 of thin tubular structures protruded from the apex of cantilever with a length of approximately 465 nm and the diameter of approximately 17.29 nm. The resultant CNTs consisted of graphite layers, implying multi-walled carbon nanotube (MWCNT) structure.

The CNT-modified cantilever was used for AFM imaging. Test sample was silicon dioxide coated with a uniform layer of platinum which is VLSI standard sample. Scan rate is at 1 Hz and scan size is at 6x6 μm^2. Line profile of the image obtained from CNT-modified cantilever showing relatively same specification as that of standard sample, while that of used and new cantilevers showed the much difference especially in mean height. CNT-modified cantilever showed 1 - 2 % difference from the standard specification while used cantilever showed 2 - 20% difference from the standard specification. These results implying that superior to new and used AFM cantilevers, the CNT-modified AFM cantilevers exhibit high-resolution imaging in both lateral and vertical resolution. Moreover, focusing at the line profile of the AFM image scanned by CNT-modified cantilever, it was found that surface of cavity showed roughness while the line profile of the AFM image scanned by new and used cantilever showed flat surface of cavity. This result indicated that CNT-modified cantilever have higher resolution than new and used AFM cantilever in term of bottom roughness. After AFM imaging, CNT still attached on the cantilever, implying durability and long life time of CNTs due to their excellent mechanical properties. These results show a potential reuse of used cantilever which will have advantages in terms of AFM imaging improvement and the company expense reduction.

Yield of CNT-modified AFM cantilever is considered into two terms. Yield of 1-2 CNTs on the apex of AFM cantilever is approximately 27 %yield (3/11) while yield of CNTs on the apex of AFM cantilever is approximately 64 %yield (7/11).

This material is reserved for educational use only, not allowed for commercial use.
Forbidden to modify the content, and cite the document when use.

For future research, to apply CNT-modified cantilever for practical application, it is required to study on life time and effect of CNT on hard disk drive surface. The strength and Young's modulus of CNT at the tip of AFM cantilever can be tested by force distance curve before imaging scanning. The resolutions of the CNT on the new cantilever and the CNT on the used cantilever should be compared. The used cantilever after growth of CNT can possibly reuse again by plasma cleaning process.

This material is reserved for educational use only, not allowed for commercial use.
Forbidden to modify the content, and cite the document when use.

REFERENCES

[1] M. S. Dresselhaus, G. Dresselhaus, Ph. Avouris, "**Carbon nanotubes; synthesis, structure, properties, and application.**", Springer, vol. 15, 2001, p. 225.

[2] H. Nejo, P. Avouris, B. Bhushan, D. Bimberg, K. Von, H. Sakakiand, and R. Wiesendanger, "**Nanostructures fabrication and analysis.**", Springer, vol. 12, 2007, p. 151.

[3] J. Robertson, G. Zhong, C. S. Esconjauregui, B. C. Bayer, C. Zhang, M. Fouquet, and S. Hofmann, "Applications of carbon nanotubes grown by chemical vapor deposition", **Applied Physics**, vol. 51, 2012

[4] M. Meyyappan, "**Carbon nanotubes science and applications.**", CRC PRESS, 2005, p. 15.

[5] H. Dai, J. H. Hafner, A. G. Rinzler, D. T. Colbert, and R. E. Smalley, "Nanotubes as nanoprobes in scanning probe microscopy.", **Nature**, vol. 384, 1996, pp. 147 - 150.

[6] M. F. Yu, M. J. Dyer, G. D. Skidmore, H. W. Rohrs, X. Lu, K. D. Ausman, J. R. Vonher, and R. S. Ruoff. "Three-dimensional manipulation of carbon nanotubes under a scanning electron microscope.", **Nanotechnology**, vol. 10, 1999, pp. 244 - 252.

[7] L. Dong, B. J. Nelson, X. Tao, L. Zhang, X. Zhang, D. R. Frutiger, and A. Subramanian, "Nanorobotic manipulation of carbon nanotubes inside transmission electron microscope.", **Proc. 4th IFAC symposium on mechatronic systems**, vol. 4, 2006, pp. 114 - 119.

[8] J. H. Hafner, C. L. Cheung and C. M. Lieber. "Growth of nanotubes for probe microscopy tips.", **Nature**, vol. 398, 1999, pp. 761 - 762.

[9] C. L. Cheung, J. H. Hafner, T. W. Odom, K. Kim, and C. M. Liebera, "Growth and fabrication with single-walled carbon nanotube probe microscopy tips.", **Applied Physics Letters**, vol. 76, 2000, pp. 3136 - 3138.

[10] P. Dulyaseree, W. Wongwiriyapan, W. Jarernboon, W. Bunjongpru, S. Sopitpan, S. Porntheeraphat, S. Ichikawa and J. Nukeaw, "Effect of support layers on growth of carbon nanomaterials by alcohol catalytic chemical vapor deposition.", **Journal of the Microscopy Society of Thailand,** vol. 1-2, 2012, pp. 90 - 93.

This material is reserved for educational use only, not allowed for commercial use.
Forbidden to modify the content, and cite the document when use.

[11] C. L. Cheung, J. H. Hafner, and C. M. Lieber, "Carbon nanotube atomic force microscopy tips: direct growth by chemical vapor deposition and application to high-resolution imaging.", **Proc. the National Academy of Sciences of the United State of America** , vol. 97, 2000, pp. 3809 - 3813.

[12] E. Yenilmez, Q. Wang, R. J. Chen, D. Wang, and H. Dai, "Wafer scale production of carbon nanotubes scanning probe tips for atomic force microscopy.", **Applied Physics Letters**, vol. 80, Feb, 2002, pp. 2225 - 2227.

[13] K. Takagahara, Y. Takei, E. Iwase, K. Matsumoto, and I. Shimoyama, "Batch fabrication of carbon nanotubes at afm probe tips and afm imaging.", **IEEE**, 2008, pp. 713 - 716.

[14] W. Wongwiriyapan, S. Honda, T. Mizuta, T. Ohmori,T. Murakami, K. Kisoda, H. Harima, J. G. LEE, H. Mori, K. Oura and M. Katayama, "Direct growth of single-walled carbon nanotubes on W tip apex.", **Japanese Journal of Applied Physics**, vol. 45, 2006, pp. 1880 - 1882.

[15] C. S. Han , Y. H. Shin, Y. H. Yoon, "Fabrication and characterization of carbon nanotube tip modified by focused ion beam.", **IEEE**, 2007, pp. 290 - 293.

[16] J. Kim, K. No, and C. J. Lee, "Growth and field emission of carbon nanotubes on electroplated Ni catalyst coated on glass substrates.", **Journal of Applied Physics**, vol. 90, 2001, pp. 2591 - 2594.

[17] M. K. Singh, P. P. Singh, E. Titus, D. S. Misra, F. Lenormand, "High density of multiwalled carbon nanotubes observed on nickel electroplated copper substrates by microwave plasma chemical vapor deposition.", **Elsevier**, vol. 354, 2002, pp. 331 - 336.

[18] http://medicine.tamhsc.edu/basic-sciences/sbtm/afm

[19] http://www.vub.ac.be/META/toestellen_AFMSTM.php

[20] http://www.parkafm.com

[21] B. Bhushan et al., "**Handbook of Nanotechnology**". Springer, vol. 3, 2010.

[22] N. A. Geisse, "AFM and combined optical techniques". **Materials Today**, vol. 12, 2011.

[23] F. J. Giessibl,"Advances in atomic force microscopy.", **Reviews of Modern Physics**, vol. 75, 2013.

[24] http://www.ntmdt.com/spm-basics/view/effect-tip-radius-cone-angle

This material is reserved for educational use only, not allowed for commercial use.
Forbidden to modify the content, and cite the document when use.

[25] S. Yellampalli et al., "**Carbon nanotubes - polymer nanocomposites.**", Intech, 2011.

[26] Jiang, X. Yu, and Aibing, "Low dimensional silver nanostructures: synthesis, growth mechanism, properties and applications", **Journal of Nanoscience and Nanotechnology**, vol. 10, 2010, pp. 7829-7875.

[27] http://ipn2.epfl.ch/CHBU/NTproduction1.htm

[28] M. Yasutake et al., "**Carbon nanotubes: properties and applications.**", CRC Press, 2006.

[29] A. D. Slattery, A. J. Blanch, J. S. Quinton, and C. T. Gibson, "Efficient attachment of carbon nanotubes to conventional and high-frequency AFM probes enhanced by electron beam processes.", **Nanotechnology**, vol. 24, 2013

[30] https://store.nanoscience.com

[31] http://nzic.org.nz/ChemProcesses/metals/8G.pdf

[32] http://www.thomasnet.com/articles/custom-manufacturing-fabricating/electro-plating-process

[33] http://www.nickelplatingkit.com/electroplating-nickel/

[34] http://www.electrolytics.org/faradaysLaw.html

[35] http://www.vcbio.science.ru.nl/public/pdf/fesem_info_eng.pdf

[36] http://en.wikipedia.org/wiki/Scanning_electron_microscope

[37] http://www.dstuns.iitm.ac.in/microscopy-instruments.php

[38] http://en.wikipedia.org/wiki/Transmission_electron_microscopy

[39] http://en.wikipedia.org/wiki/Raman_spectroscopy

[40] Mordechay Schlesinger and Milan Paunovic, "**Modern electroplating.**", John Wiley & Sons, Inc., vol. 5, 2010, pp. 79 - 114.

[41] Ayala, P. Reppert, J. Grobosch, M. Knupfer, M. Pichler, T. Rao, A. M, "Evidence for substitutional boron in doped single-walled carbon nanotubes.", **Applied Physics Letters**, vol. 96, 2010, p. 183110.

[42] http://www.sixsigmatraining.org/six-sigma-projects/how-to-calculate-process-yields.html

This material is reserved for educational use only, not allowed for commercial use.
Forbidden to modify the content, and cite the document when use.

ACHIEVEMENTS

(1) Y. Maneerat, P. Dulyaseree and W. Wongwiriyapan

Modification of used Atomic Force Microscope Cantilever by Carbon Nanotube Attachment and its Imaging Performance

Proceedings of the 8th Annual Conference of Thai Physics Society, Chiangmai, Thailand, March 21-23, 2013

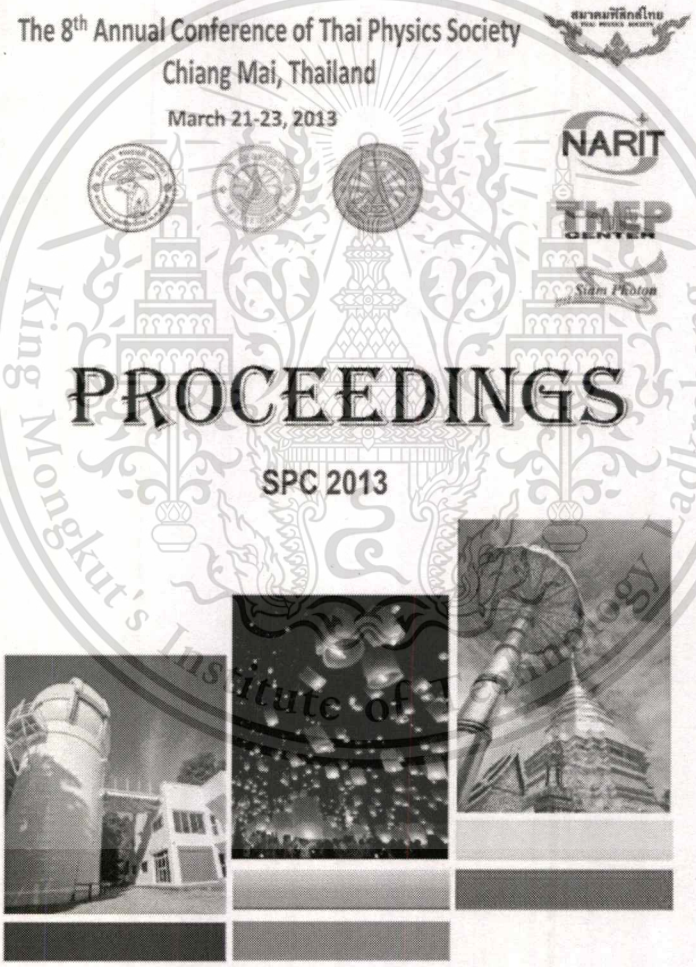

This material is reserved for educational use only, not allowed for commercial use.
Forbidden to modify the content, and cite the document when use.

March 23rd, 2013 Location: CGV 2-3				
	CGV 3-2	**CGV 2-2**	**CGV 3-1**	**CGV 2-1**
	Astrophysics and Cosmology & High energy and Particle Physics	**Condensed Matter Physics & Atomic Physics Quantum Physics, Molecular and Chemical Physics**	**Material Physics, Nanoscale Physics and Nanotechnology**	**Student Competition (Special Project)**
	Session Chair: Prof.Dr.Yupeng Yan (SUT)	**Session Chair: Asst. Prof. Dr.Jiraroj T-Thienprasert (KU)**	**Session Chair: Assoc. Prof. Dr. Supon Ananta (CMU)**	**Session Chair: Assoc. Prof. Dr. Prayoon Songsiriritthigul (SUT)**
9:00 - 9:30	Invited_31: Burin (CU)	Invited_24: Feng Yuan Ping (NUS)	Invited_26: Pisith (CMU)	
9:30 - 10:00	Invited_23: Warintorn (SUT)	Invited_25: Sirichok (SUT)	Invited_27: Anuson (UbU)	
10:00 - 10:30	HEP_O01, HEP_O02	Atom-QM_O01, Atom-QM_O02	Mat-Nano_O05, Mat-Nano_O06	
10:30 - 10:45	Coffee Break			
	Astrophysics and Cosmology & High energy and Particle Physics	**Condensed Matter Physics & Surface, Interface and Thin Films**	**Material Physics, Nanoscale Physics and Nanotechnology**	
	Session Chair: Dr. Siramas Komonjinda (CMU)	**Session Chair: Assoc. Prof. Dr. Kajornyod Yoodee (CU)**	**Session Chair: Prof. Dr. Santi Maensiri (SUT)**	
10:45 - 11:15	Invited_28: Piyabut (CU)	Invited_29: Yongyut (CMU)	Invited_30: Wisanu (KMITL)	
11:15 - 11:45	HEP_O03, HEP_O04	Surf-Films_O01, Surf-Films_O02	Mat-Nano_O07, Mat-Nano_O08	
11:45 - 12:15	HEP_O05, HEP_O06	Surf-Films_O03, Surf-Films_O04	Mat-Nano_O09, Mat-Nano_O10	
12:15 - 13:15	Lunch			

This material is reserved for educational use only, not allowed for commercial use.
Forbidden to modify the content, and cite the document when use.

Modification of Used Atomic Force Microscope Cantilever by Carbon Nanotube Attachment and its Imaging Performance

Y. Maneerat[1*], P. Dulyaseree[2], S. Pratontep[2,3] and W. Wongwiriyapan[2,3]

[1]*College of Data Storage Innovation, King Mongkut's Institute of Technology Ladkrabang, Chalongkrung Rd, Ladkrabang, Bangkok 10520 Thailand*
[2]*College of Nanotechnology, King Mongkut's Institute of Technology Ladkrabang, Chalongkrung Rd, Ladkrabang, Bangkok 10520 Thailand*
[3]*Nanotec-KMITL Center of Excellence on Nanoelectronic Devices, Chalongkrung Rd, Ladkrabang, Bangkok 10520 Thailand*
**Corresponding author. E-mail: Yuwapan.Maneerat@Seagate.com*

Abstract

Modification of used atomic force microscope (AFM) cantilever by carbon nanotube (CNT) attachment and its imaging performance was demonstrated. CNTs were directly grown on apex of used AFM cantilever by Ni catalyst-assisted chemical vapor deposition (CVD) using ethanol as carbon source. To obtain CNTs protruding from the apex of the pyramid shape of cantilever, the optimum CVD was operated at growth temperature of 850^{0}C for 20 min. Field-emission electron microscope, transmission electron microscope and Raman spectroscopy were utilized for the synthesized CNT characterization. For imaging performance test, silicon dioxide coated with a uniform layer of platinum which is AFM standard sample, was used as a test sample. Surpassing new and used AFM cantilevers, imaging obtained from CNT-modified AFM cantilever showed high-resolution imaging in both lateral and vertical resolution.

Keywords: Carbon nanotube, Chemical vapor deposition, Atomic force microscope, Cantilever

Introduction

Atomic force microscope (AFM) is an important tool for matter imaging, measuring, and manipulating. Recently, with the development of nanotechnology, carbon nanotube (CNT) is considered as an ideal structure probe used for scanning probe microscopes due to its excellent structural, mechanical, and electrical properties [1]. The key advantages of CNT over conventional microfabricated Si cantilever include high lateral imaging resolution due to tip sharpness, high imaging consistency over prolonged operation, and high durability and long lifetime due to its excellent mechanical stiffness and high resilience against mechanical damage [1]. To fabricate the CNT cantilever, CNT will be attached to the apex of the pyramid shape of cantilever by bonding CNT using an acrylic adhesive [2] or growing CNT directly on the cantilever apex by chemical vapor deposition (CVD) [3-6]. Direct growth provides a good mechanical contact between CNT and the cantilever body. From previous reports, CNT cantilevers mostly demonstrate on the new Si cantilever. However, in term of performance cost, modification of used AFM cantilever for imaging improvement is a challenge.

In this study, the used cantilever was used as a platform for CNT attachment by direct growth method of Ni catalyst-assisted CVD using ethanol as carbon source. Surpassing new and used AFM cantilevers, imaging obtained from CNT-modified AFM cantilever showed high-resolution imaging in both lateral and vertical resolution.

Materials and Methods

AFM cantilever which could not be longer used for imaging scanning, used cantilever, was modified by attachment of CNT on its apex. Attachment of CNT was conducted by direct growth of CNT on the pyramid shape of the cantilever using Ni catalyst-assisted CVD. Ni catalyst layers were deposited on the cantilever using electroplating technique. Next, Ni catalyst layer-deposited AFM cantilever was set into a quartz tube reactor for CVD process. Detailed

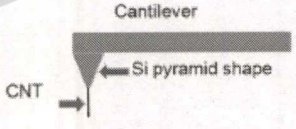

Figure 1 Schematic view of CNT-modified cantilever

This material is reserved for educational use only; not allowed for commercial use.
Forbidden to modify the content, and cite the document when use.

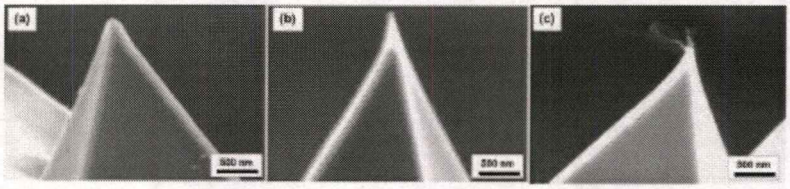

Figure 2 FESEM images of (a) reused, (b) new and (c) CNT-modified cantilevers

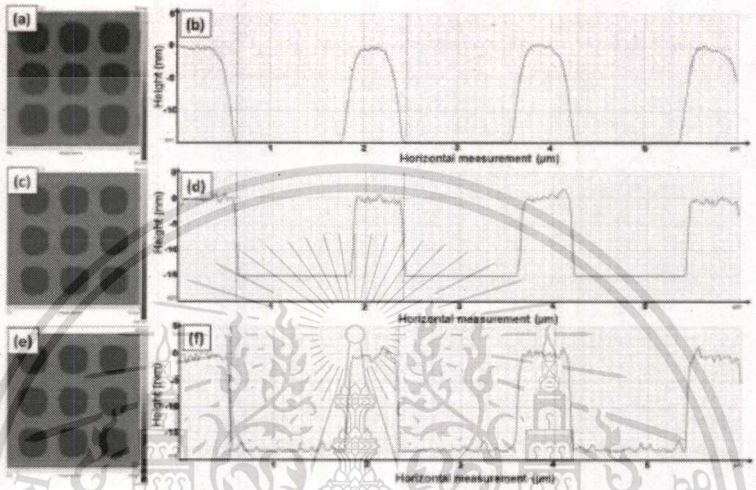

Figure 3 AFM images and its line profile using (a), (b) reused, (c), (d) new and (e), (f) CNT-modified AFM tips, respectively. Scan area is 6μm x 6 μm.

Table 1 Average of mean height, mean pitch and angle of AFM image scanned by different cantilevers

	Mean Height, Z (nm)	Mean Pitch, X (μm)	Mean Pitch, Y (μm)	Angle (degree)
Standard sample	18.400± 3.300	1.799± 0.023	1.799± 0.023	90.00°
Used cantilever	14.632± 0.185	1.817± 0.023	1.830± 0.016	97.61° ± 1.37
New AFM cantilever	15.148± 0.269	1.804± 0.017	1.830± 0.014	93.62° ± 2.23
CNT-Modified cantilever	18.568± 0.315	1.803± 0.013	1.822± 0.015	92.02° ± 1.63

experiment is described elsewhere [7]. Shortly, the quartz tube was filled with Ar gas at a flow rate of 500 sccm until the temperature reached to 850°C. Ethanol vapor (99.99%) was switched into the furnace by Ar bubbling at a flow rate of 125 sccm for 20 min. Field-emission electron microscope (FESEM, FEI, Sirion NPGS V9), high resolution transmission electron microscope (HRTEM, FEI, Tecnai G2 20) and Raman spectroscopy (Thermo Scientific, DXR Smart Raman) were utilized for the synthesized CNTs characterization.

For AFM imaging performance test, the CNT modified cantilever was used to scan silicon dioxide coated with a uniform layer of platinum which is AFM standard sample (VLSI standard sample, STS2-180P). Atomic force microscopy (BRUKER, Dimension Icon) was utilized for AFM imaging in tapping mode. For comparison, new and used cantilevers were also employed for imaging scanning.

Results and Discussion

Figure 1 shows a schematic view of CNT-modified cantilever. Figures 2(a)-(c) show FESEM

This material is reserved for educational use only, not allowed for commercial use.
Forbidden to modify the content, and cite the document when use.

images of used, new and CNT-modified cantilevers, respectively. The curvature radius of each cantilever apex was different. Used cantilever had the dull apex with a curvature radius of 145 nm, while new cantilever had the relatively sharp apex with a curvature radius of 58 nm. For CNT-modified cantilever, CNTs with a thin tubular structure were protruded from apex of cantilever with a length of approximately 465 nm. The curvature radius of the used cantilever before CNT modification was approximately 87 nm.

For HRTEM observation, it is hardly to directly observe the structure of CNT protruded from cantilever apex. To obtain the trend of the resultant CNTs, CNTs on cantilever was removed to Cu grid and characterized. Thus, not only the CNTs at the apex, but also CNTs at the cantilever body were observed. It was found that the resultant CNTs consisted of multi-graphene layers, implying multi-walled carbon nanotube (MWCNT) structure. Diameters of MWNTs were approximately estimated to be with a diameter of 17.29±0.59 nm (data not shown).

In order to demonstrate the imaging performance of the CNT-modified cantilever, silicon dioxide coated with a uniform layer of platinum (VLSI Standard sample, STS2-180P) which is AFM standard sample was used as a test sample. The specification of the stand sample was shown in Table 1. Its mean height, mean pitch (x,y) and angle are 18.400±3.300 nm, 1.799 μm±0.023 μm and 90°, respectively. For imaging scanning, each cantilever was scanned under the same AFM operation setting at a scan rate of 1 kHz, set point of 250 mV, scan size of 6 μm x 6 μm, samples/line of 512 and scan angle of 90°. Scanning was conducted for 2 times for each cantilever. Figures 4(a)-4(f) show AFM images of standard sample and its line profile obtained from used, new and CNT-modified AFM tip, respectively. From figures 4(a), 4(c) and 4(e), it can be obviously seen that the imaging from new and CNT-modified cantilever was clear, while the imaging from used cantilever was vague. Average of mean height, mean pitch and angle of each image were measured from its line profile of 9 pitches and were summary in Table 1. Line profile of the image obtained from CNT-modified cantilever showing relatively same specification as that of standard sample, while that of used and new cantilevers showed the small difference in mean height, implying that surpassing not only used cantilever but also new cantilever, the CNT-modified cantilever showed better resolution imaging in both lateral and vertical resolution. After imaging, the CNT-modified cantilever was observed by FESEM again. The CNT still attached on the cantilever, showing its good mechanical contact with cantilever (data not shown).

Conclusions

The used AFM cantilever was modified by attachment of CNT. CNT was synthesized by CVD method using ethanol as carbon source. After optimum CVD condition, MWNTs were attached at the apex of pyramid shape of cantilever. Silicon dioxide coated with a uniform layer of platinum which is AFM standard sample was used as a sample for AFM imaging. Surpassing new and used AFM cantilevers, imaging obtained from CNT-modified cantilever showed high-resolution imaging in both lateral and vertical resolution. These results show a potential reuse of used cantilever which will have advantages in terms of AFM performance and cost.

Acknowledgments

The author would like to acknowledge HGSA Failure Analysis Laboratory, Seagate (Thailand) Co., Ltd. (KORAT) for the AFM facilities, used cantilevers and AFM standard sample supports. This work has partially supported by the National Nanotechnology Center (NANOTEC), NSTDA, Ministry of Science and Technology, Thailand, through its program of Center of Excellence Network. We also acknowledge the financial support through Master Degree Program Development in HDD Engineering Technology, NSTDA-KMITL-SEAGATE. We thank to Assoc. Prof. Dr. Vittaya Amornkitbamrung and Ms. Phikun Ratphonsan, KhonKaen University for their partly assistance in HRTEM observation.

References

1. M. S. Dresselhaus, G. Dresselhaus and Ph. Avouris, "Carbon Nanotubes; Synthesis, Structure, Properties, and Application", Springer, Berlin, (2001).
2. H. Dai, J. H. Hafner, A. G. Rinzler, D. T. Colbert and R. E. Smalley, "Nanotubes as Nanoprobes in Scanning Probe Microscopy", Nature 384 (1996) 147.
3. J. H. Hafner, C. L. Cheung and C. M. Lieber, " Growth of Nanotubes for Probe Microscopy Tips", Nature 398 (1999) 761.
4. C. L. Cheung, J. H. Hafner, T. W. Odom, K. Kim, and C. M. Lieber, "Growth and Fabrication with Single-Walled Carbon Nanotube Probe Microscopy Tips" Applied Physics Letters, 76 (2000), 3136.
5. Y. Erhan, W. Qian, Robert J. Chen, W. Dunwei and D. Hongjie, "Wafer scale production of carbon nanotubes scanning probe tips for atomic force microscopy", Applied Physics Letters, 80 (2002), 2225.
6. K. Takagahara, Y. Takei, E. Iwase, K. Matsumoto, and I. Shimoyama, "Batch Fabrication of Carbon Nanotubes at AFM Probe Tips and AFM Imaging", Proceedings of Micro

This material is reserved for educational use only, not allowed for commercial use.
Forbidden to modify the content, and cite the document when use.

Electro Mechanical Systems, 2008, IEEE 21st International Conference on (2008), 713.
7. P. Dulyaseree, W. Wongwiriyapan, W. Jaremboon, W. Bunjongpru, S. Sopitpan, Pornthreeraphat, S. Ichikawa and J. Nukeaw, "Effect of Support Layers on Growth of Carbon Nanomaterials by Alcohol Catalytic Chemical Vapor Deposition", Journal of the Microscopy Society of Thailand 6 (2012), accepted.

King Mongkut's Institute of Technology Ladkrabang

This material is reserved for educational use only, not allowed for commercial use.
Forbidden to modify the content, and cite the document when use.

AUTHOR BIOGRAPHY

Name-Surname: Ms. Yuwapan Maneerat

Date of Birth: March 8th, 1981

Present Address: 1549 Mukkamontri Rd., Muang District, Nakhonratchasima, Thailand 30000

Education: 2000-2004: Bachelor degree in Science, Majoring in Physics, Khon Kaen university

Scholarships: 2010-2012 Scholarship for study in Master of Engineering in Data Storage Technology (English program) by NSTDA, KMITL and Seagate Technology (Thailand) Ltd.

Achievements: Y. Maneerat., "Modification of Used Atomic Force Microscope Cantilever by Carbon Nanotube Attachment and its Imaging Performance", Siam Physics Congress SPC2013 Thai Physics Society on the Road to ASEAN Community 21-23 March 2013

Work Experience:

2004-2006	Thai Power Operation Company - Distributed Control System
2006-2006	Hitachi Global Storage Technology (Thailand) Company - Material Planner
2006-2008	Western Digital (Thailand) Company - Reliability Test Engineer
2008-Present	Seagate Technology (Thailand) Company - Recording Head Failure Analysis Engineer

This material is reserved for educational use only, not allowed for commercial use.
Forbidden to modify the content, and cite the document when use.